MEMBER OF BASQUE RESEARCH & TECHNOLOGY ALLIANCE

Spintronics with low-symmetry materials

Online SPICE-SPIN+X Spintronics Seminar

Oct. 25th, 2023

Fèlix Casanova

Nanodevices group, CIC nanoGUNE

San Sebastian, Basque Country (Spain)

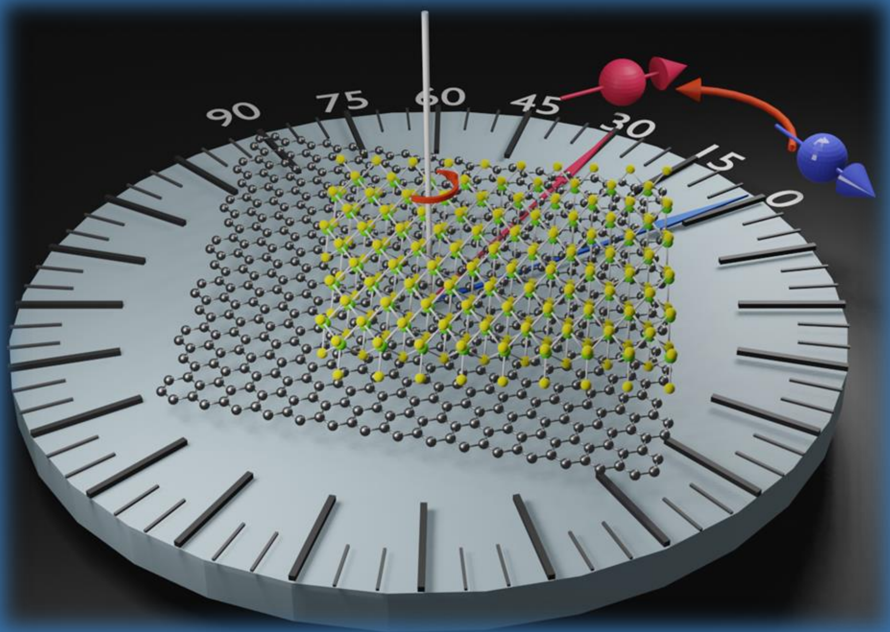

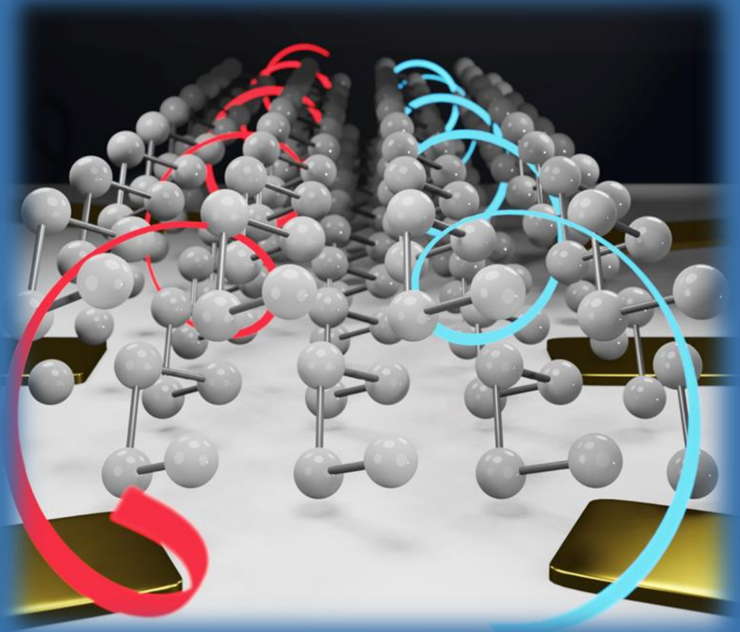


San Sebastian

NANODEVICES GROUP @ CIC NANOGUNE

INTRODUCTION: MOORE'S LAW

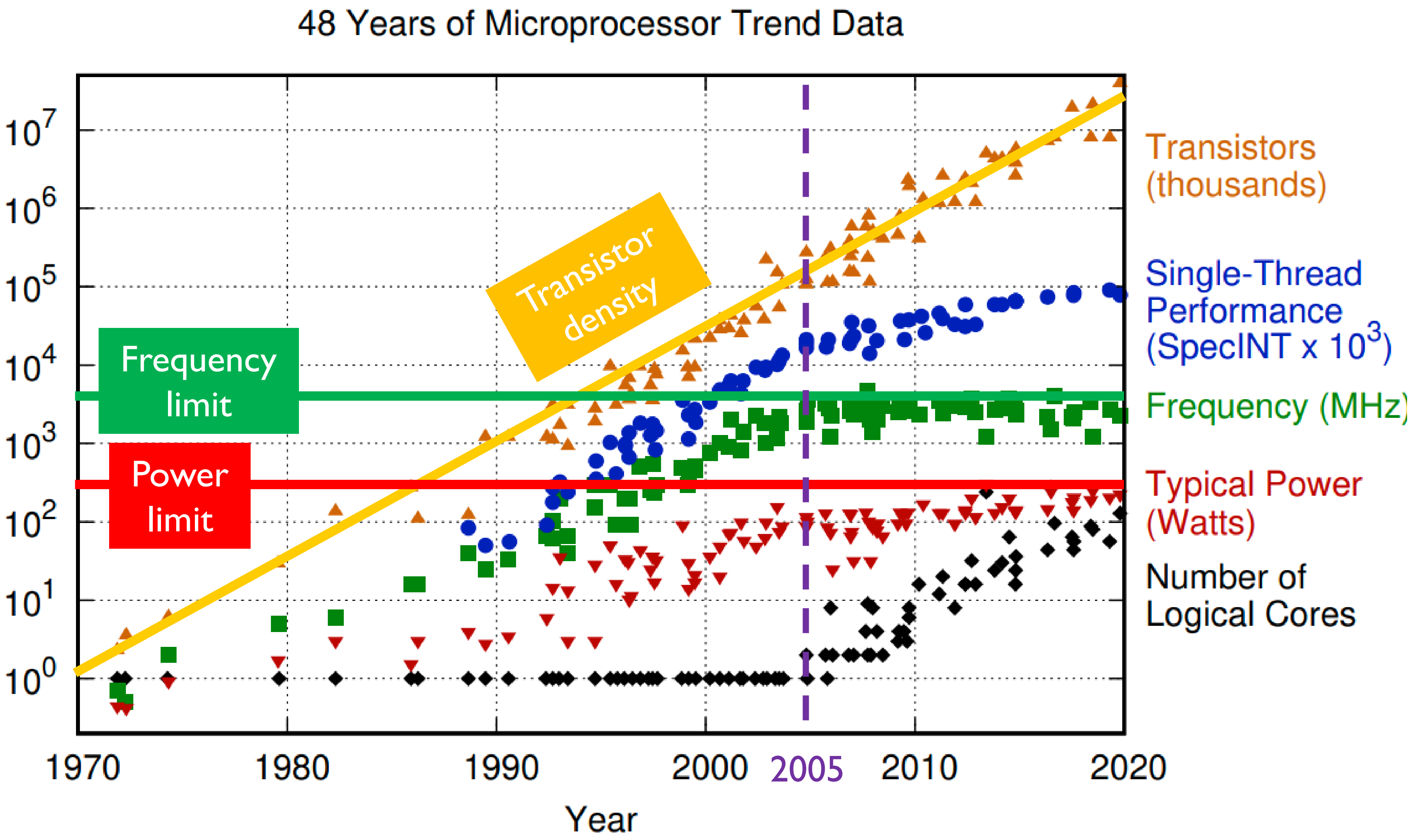

Original data up to the year 2010 collected and plotted by M. Horowitz, F. Labonte, O. Shacham, K. Olukotun, L. Hammond, and C. Batten
New plot and data collected for 2010-2019 by K. Rupp

INTRODUCTION: POWER CONSUMPTION OF ICT

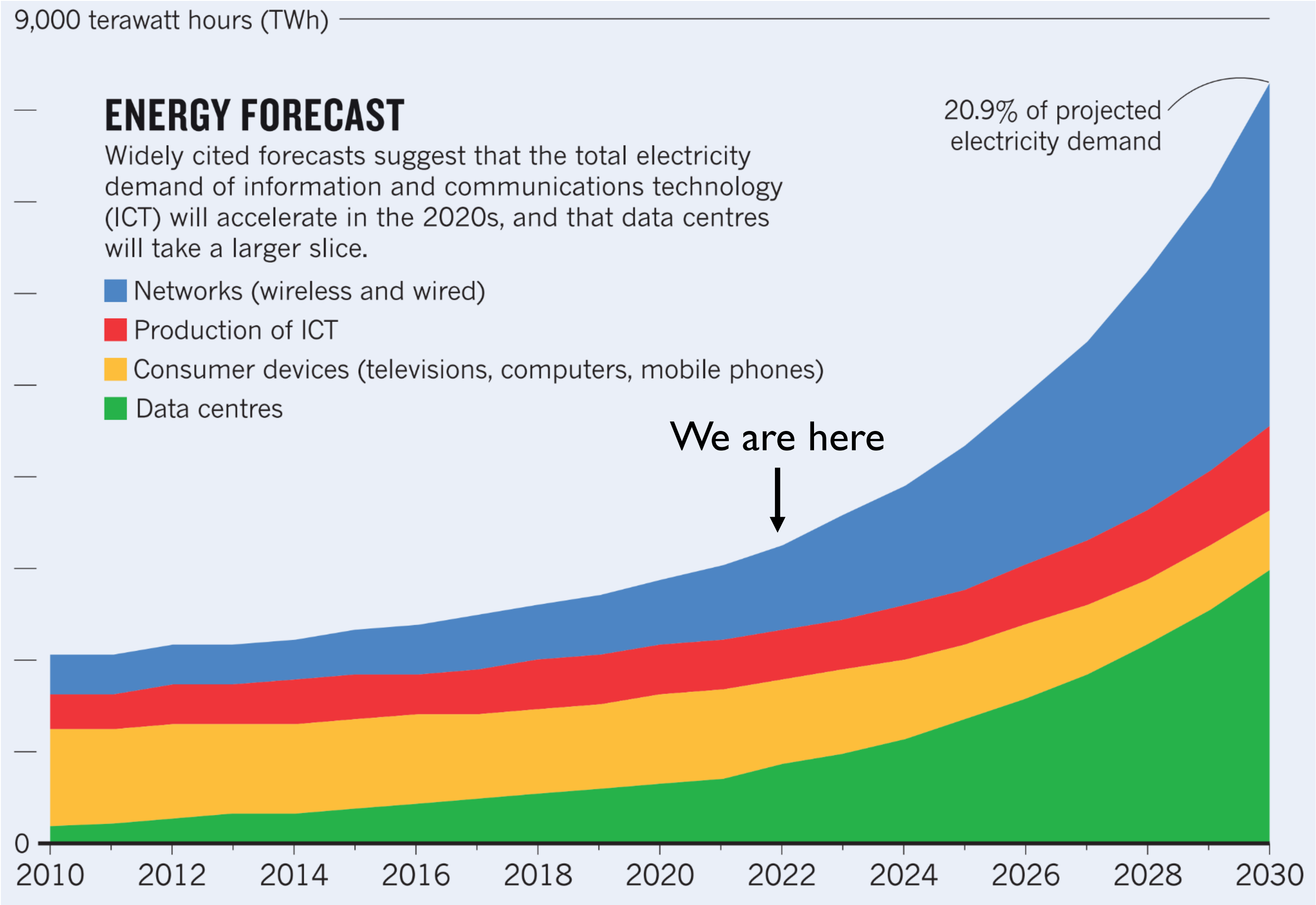

Andrea and Edler; Challenges **6**, 117 (2015); N. Jones, Nature **561**, 163 (2018)

INTRODUCTION: spintronics

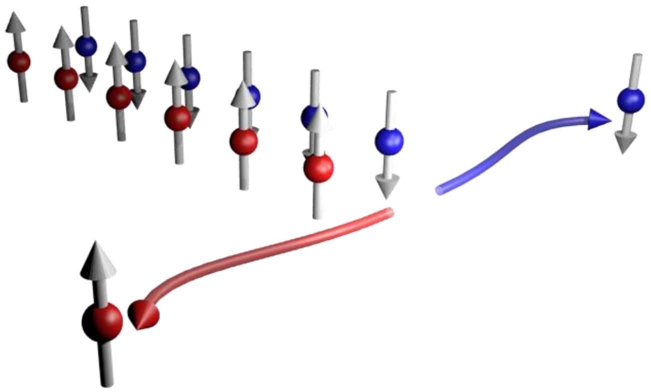

- ✓ New generation of spintronic devices that use **pure spin currents**
- ✓ Integration of memory and logic
- ✓ High speed, low power operation at reduced scale

Some spin-based logic proposals:

Spin-based magnetologic

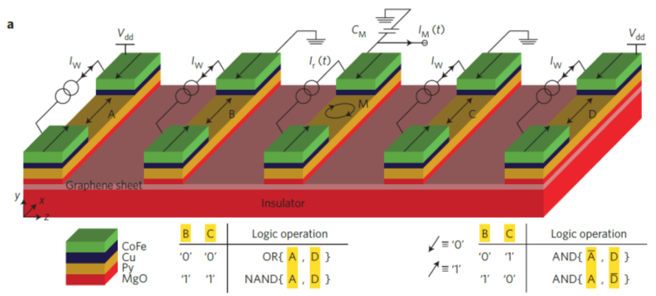

H. Dery et al. , Nature **447**, 573 (2007)
H. Dery et al. , IEEE Trans. Electr. Dev. **59**, 259 (2012)

All-spin logic

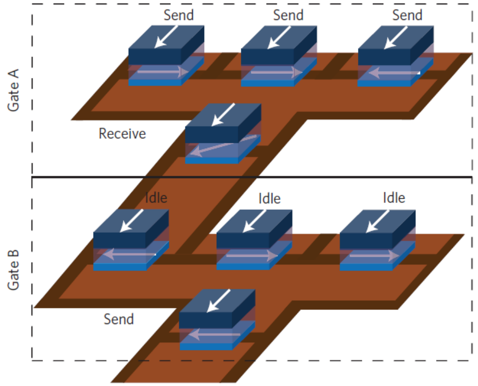

B. Behin-Aein et al., Nature Nano **5**, 266 (2010)

Magneto-electric spin-orbit logic

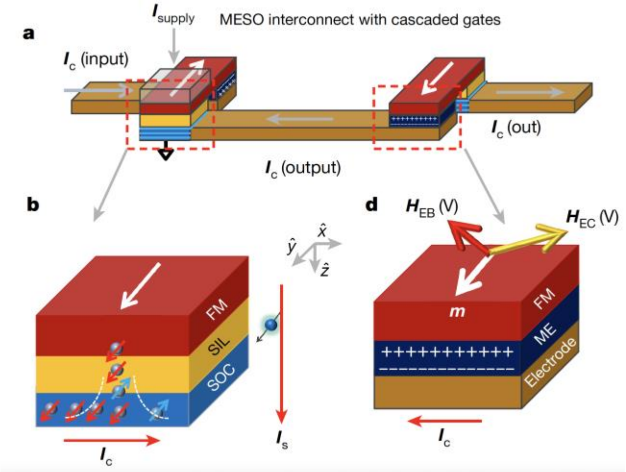

S. Manipatruni et al., Nature **565**, 35 (2019)

INTRODUCTION: spin Hall effect

✓ Strong spin-orbit coupling materials

Direct effect **(SHE)**

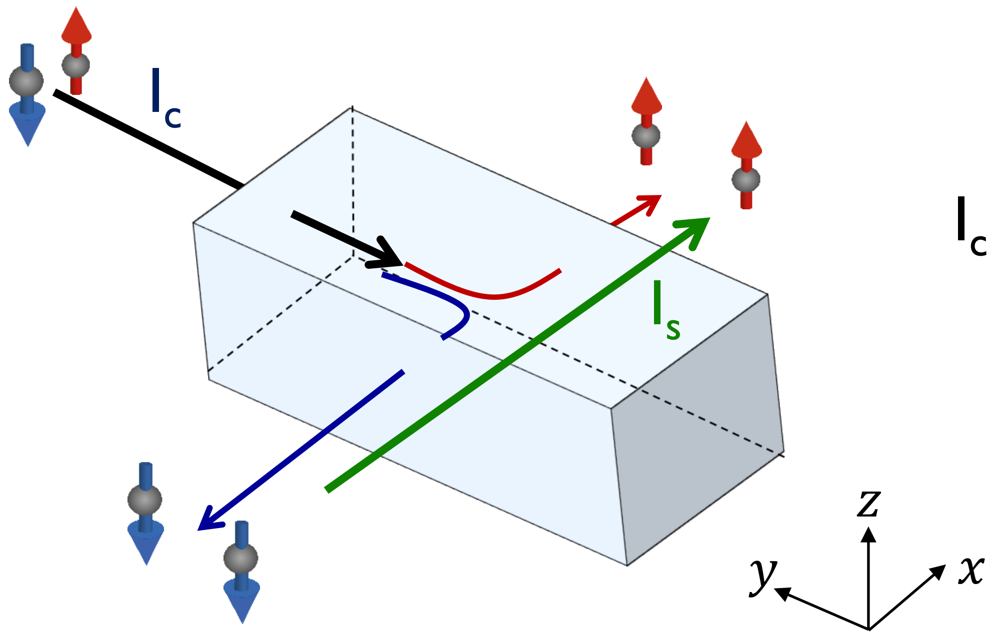

Spin current generation

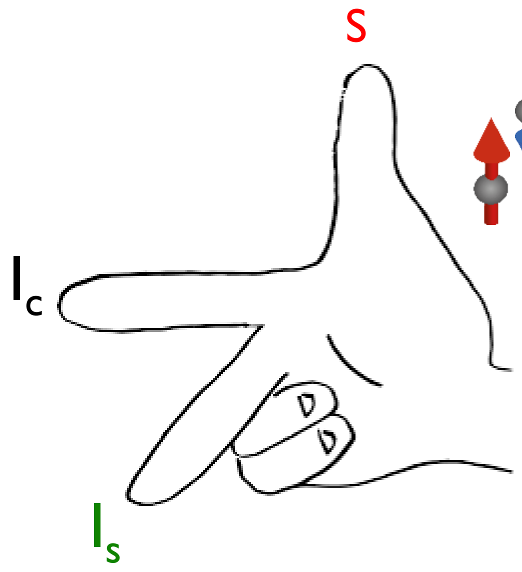

$$\boxed{\vec{j_s} = \left(\frac{\hbar}{e}\right)\theta_{SH}\,\vec{j_c} \times \vec{s}}$$

Inverse effect **(ISHE)**

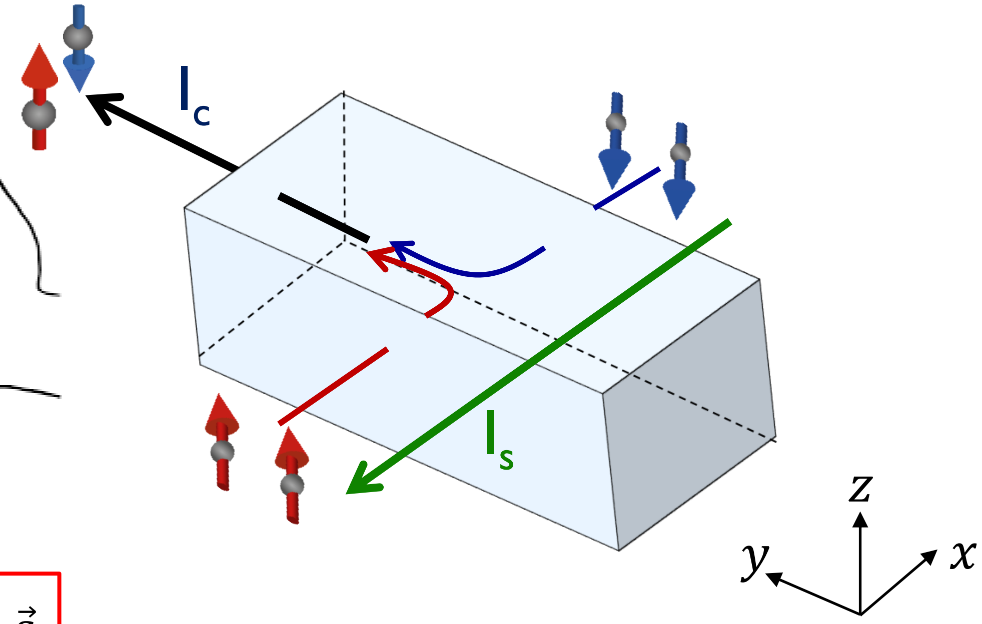

Spin current detection

INTRODUCTION: spin Hall effect

Spin Seebeck effect

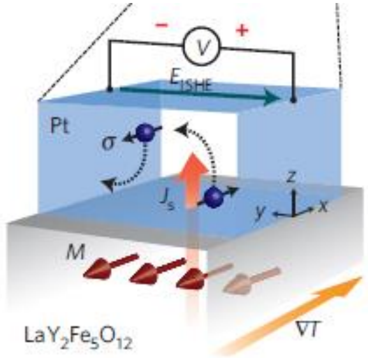

K. Uchida et al., Nature Mater. **9**, 894 (2010)

Spin Pumping

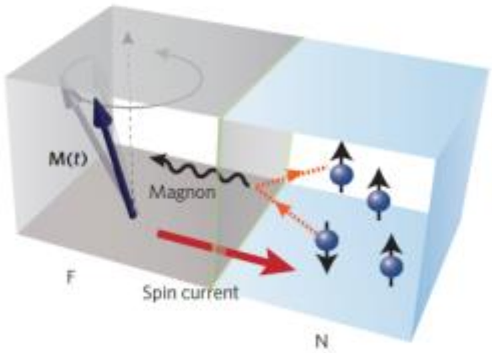

E. Saitoh et al., Appl. Phys. Lett. **88**, 182509 (2006)

Spin Hall Magnetoresistance

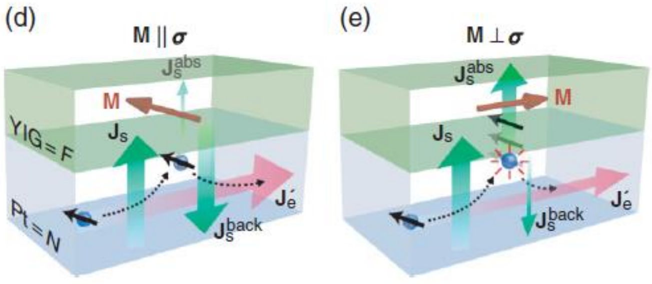

H. Nakayama et al., Phys. Rev. Lett. **110**, 206601 (2013)

Spin-orbit torques for MRAM

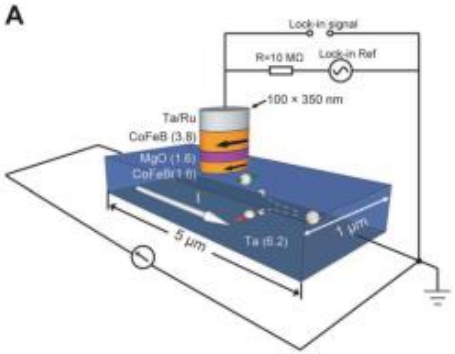

M. Miron et al., Nature **476**, 189 (2011)
L. Lui et al., Science **336**, 555 (2012)

Spin-orbit readout for MESO

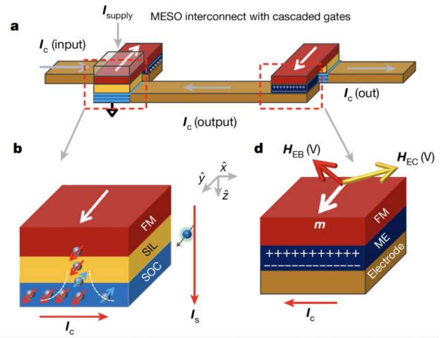

S. Manipatruni et al., Nature **565**, 35 (2019)
V.T. Pham, FC et al., Nature Electron. **3**, 309 (2020)
D. C. Vaz, FC et al., arXiv:2302.12162

INTRODUCTION: spin-orbit device for magnetic readout

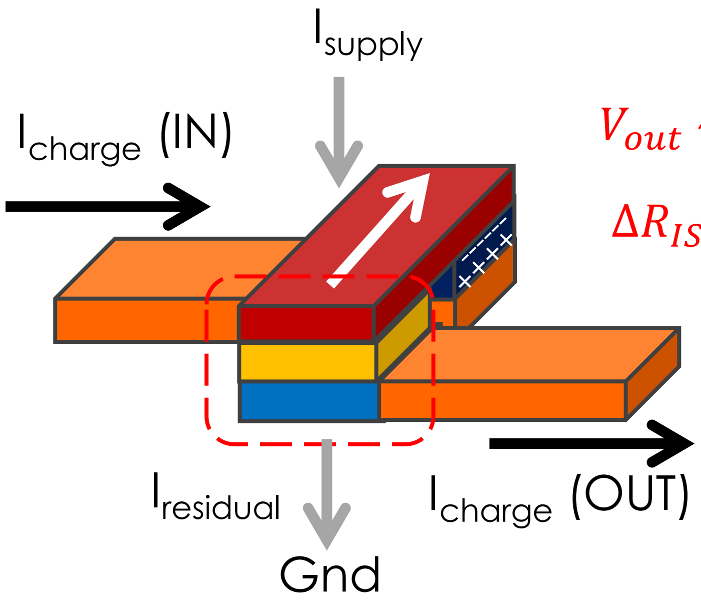

$V_{out} \sim 100\ \mathrm{mV}$

$\Delta R_{ISHE} \sim 1\ \mathrm{k\Omega}$

S. Manipatruni et al., Nature **565**, 35 (2019)

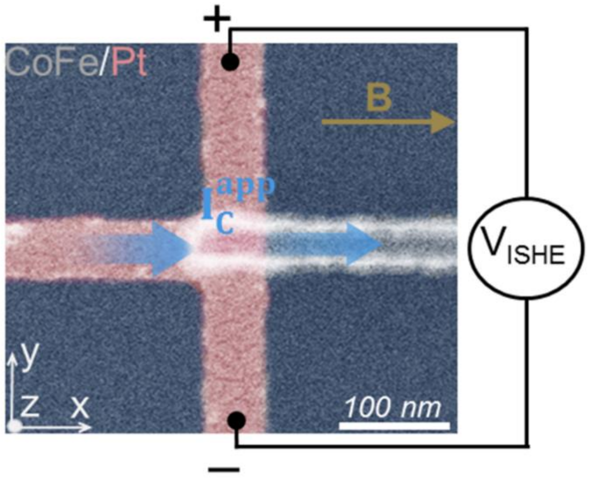

$$R_{ISHE} = \frac{V_{ISHE}}{I_C^{app}}$$

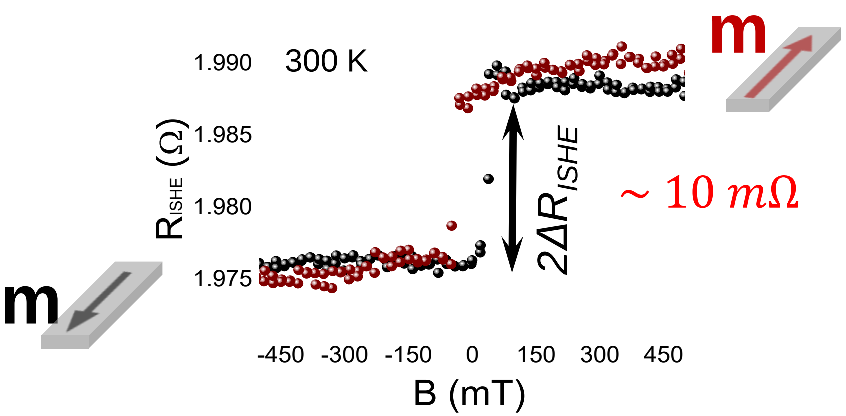

$$\Delta R_{ISHE} = \frac{1}{\left(\frac{t_{FM}}{\rho_{FM}} + \frac{t_{SOM}}{\rho_{SOM}}\right) w_{SOM}} \times \frac{P_{FM}\theta_{SH}\lambda_{SOM}}{1 + \frac{\lambda_{SOM}\rho_{SOM}}{\lambda_{FM}\rho_{FM}^{*}}}$$

V. T. Pham, FC *et al.*, Nature Electron. **3**, 309 (2020)

INTRODUCTION: spin-orbit device for magnetic readout

- ✓ **Weak** spin-orbit coupling leads to long distance spin transport (λ_{SOM})

  Elliott-Yafet dominates spin relaxation in Pt: $\lambda_{SOM} = cnt.\frac{1}{\rho_{Pt}}$

- ✓ **Strong** spin-orbit coupling leads to large spin Hall effect (θ_{SH})

  In the intrinisc (moderately dirty) regime in Pt: $\theta_{SH} = cnt.\times \rho_{Pt}$

- ✓ Mutually exclusive properties in one material

Prototypical heavy metal (Pt)
$\theta_{SH}\lambda_{SOM}$ = 0.2 – 0.4 nm

E. Sagasta, FC *et al.*, Phys. Rev. B **94**, 060412(R) (2016)

Spin-to-charge conversion with low-symmetry materials

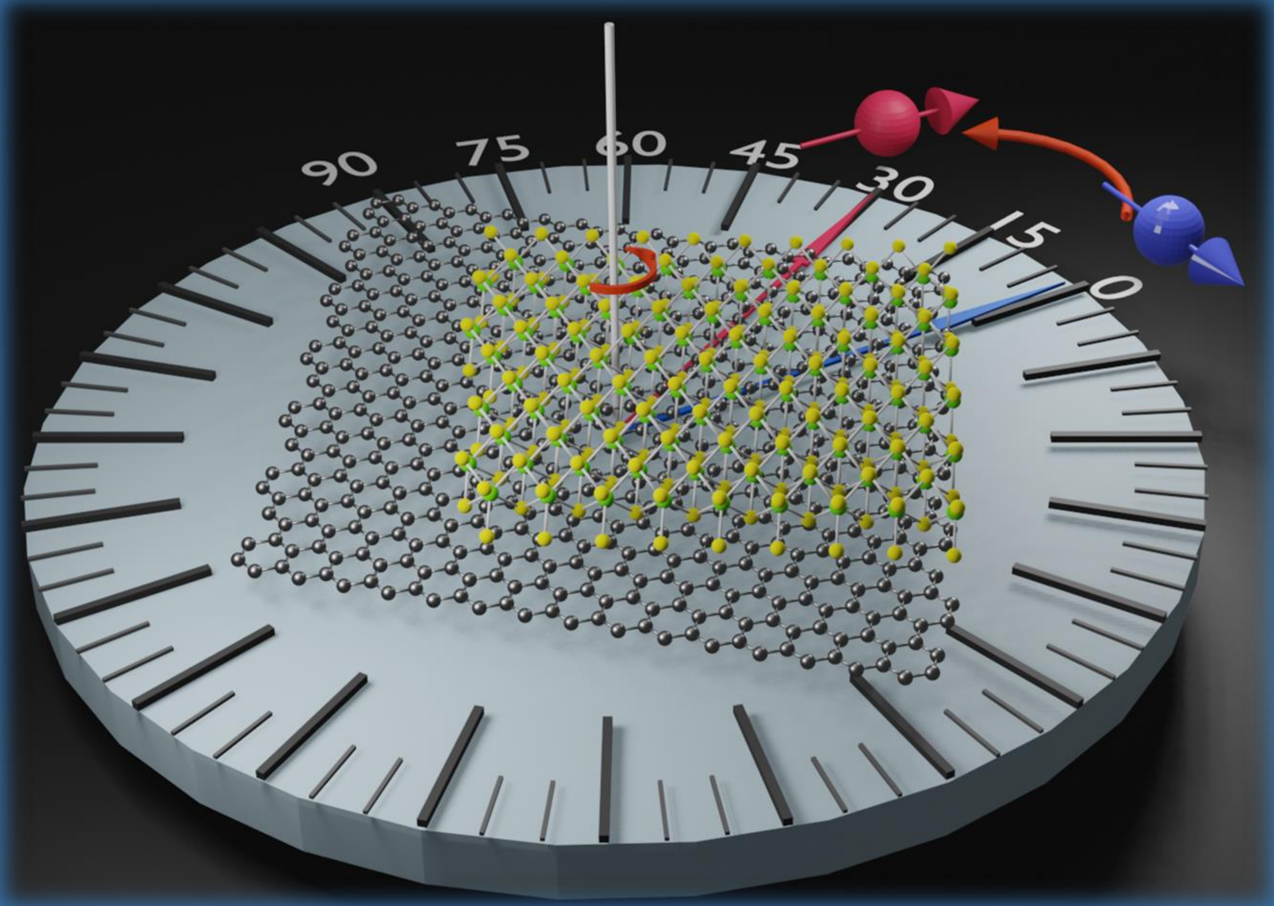

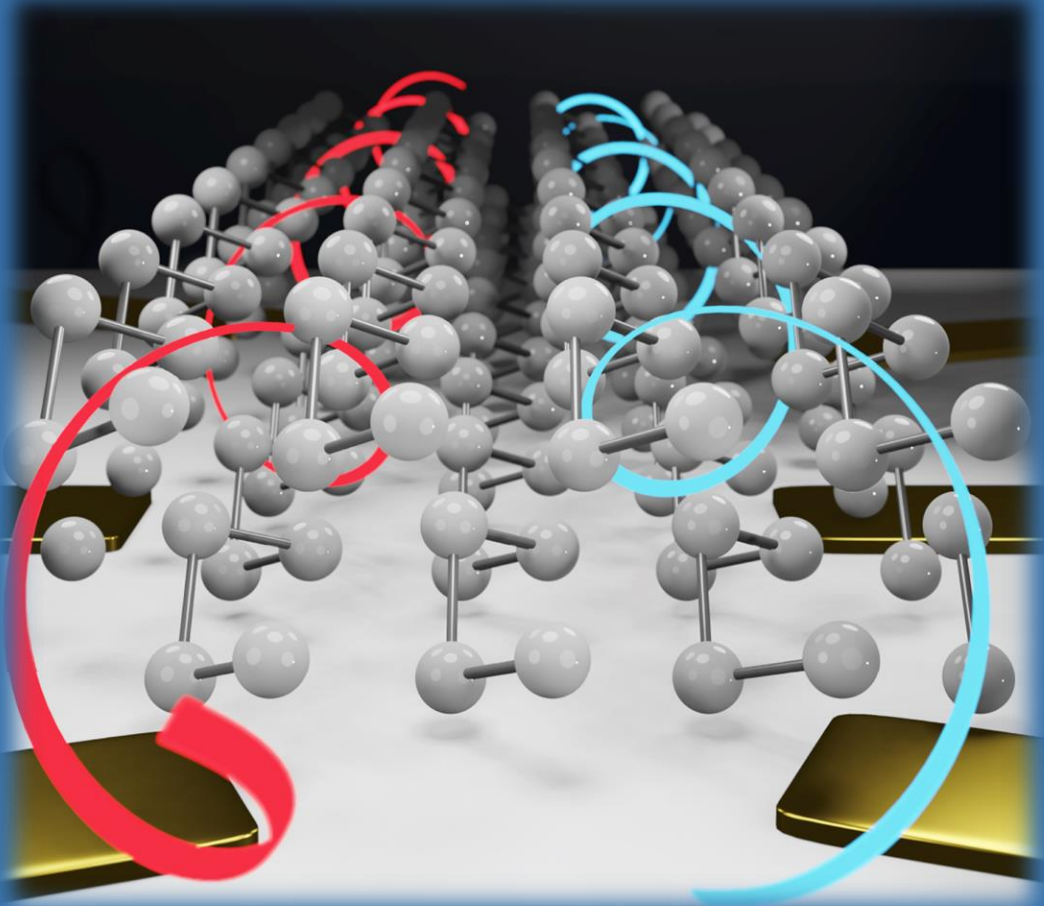

van der Waals heterostructures

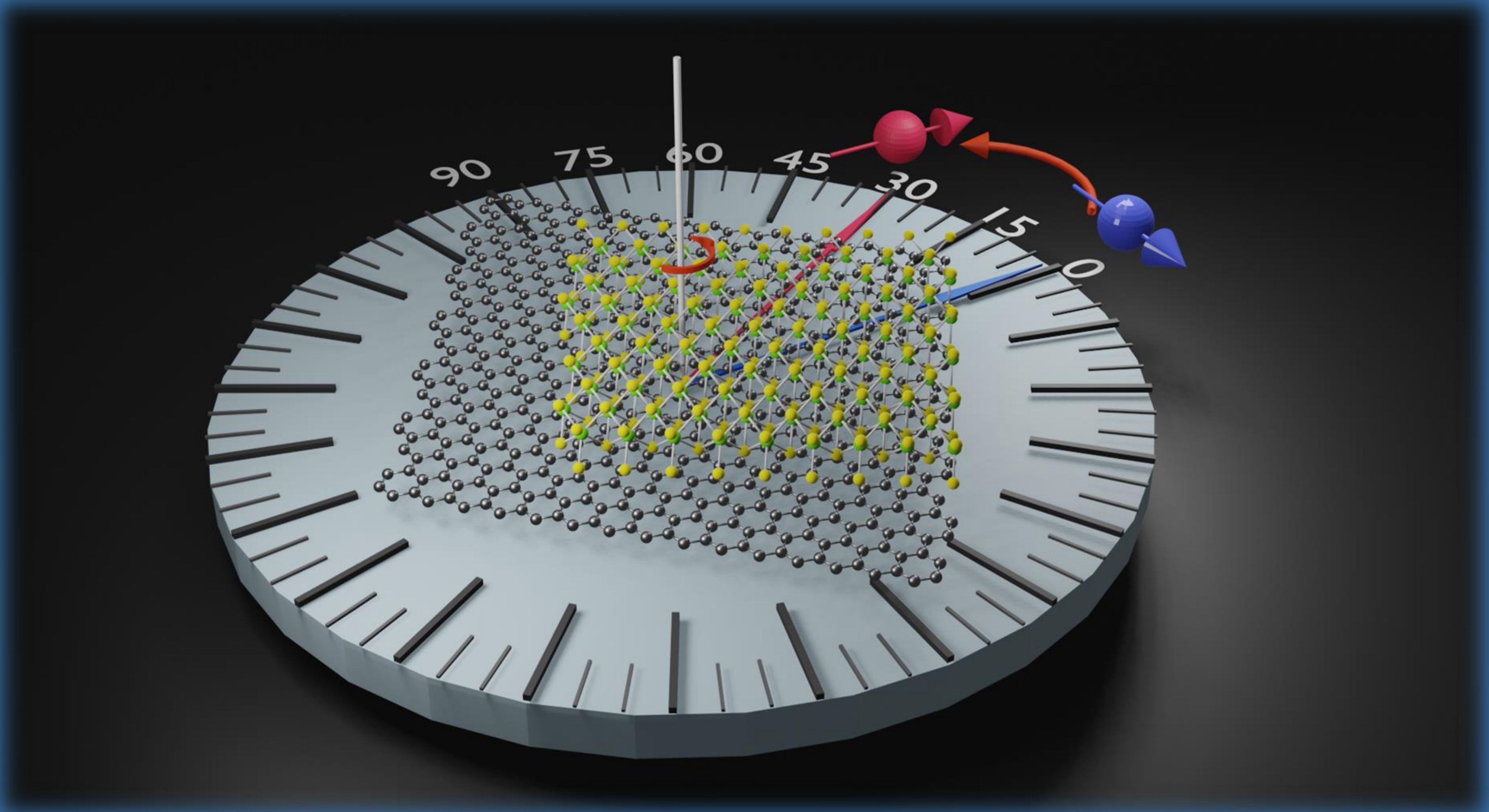

INTRODUCTION: spintronics in graphene

☑ Long distance spin transport at RT
☒ Weak spin-orbit coupling

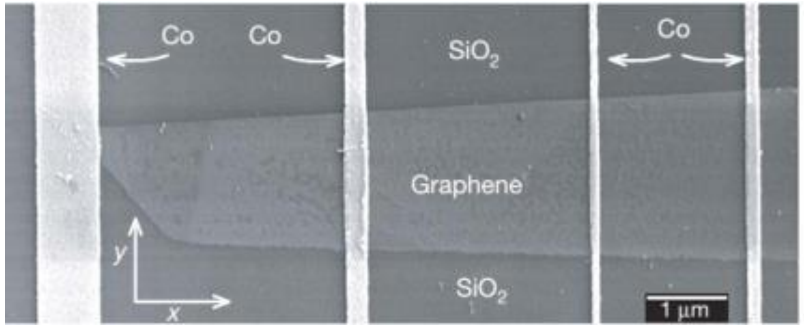

λ_s ~ 2–30 µm

N. Tombros et al., Nature **448**, 571 (2007)
B. Dlubak et al., Nature Phys. **8**, 557 (2012)
M.V. Kamalakar et al., Nature Comms. **6**, 6766 (2015)
J. Ingla-Aynés et al., Nano Lett. **16**, 4825 (2016)
M. Drögeler et al., Nano Lett. **16**, 3533 (2016)

☑ Enhanced spin-orbit coupling <u>in</u> graphene

- Hydrogenation

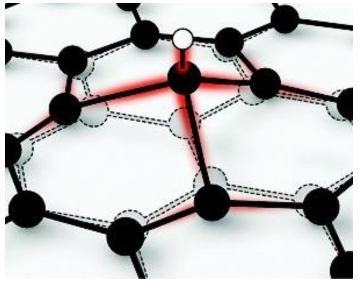

- Atomic decoration

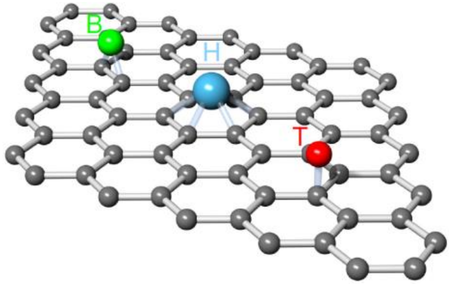

- Spin-orbit proximity

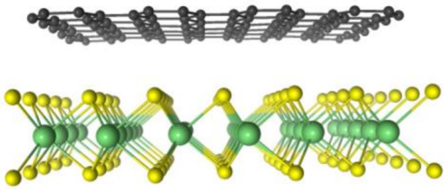

M. Gmitra et al., Phys. Rev. Lett. **110**, 246602 (2013)
C. Weeks et al. Phys. Rev. X **1**, 021001 (2011)
M. Gmitra et al. , Phys. Rev. B **93**, 155104 (2016)

INTRODUCTION: spin-orbit proximity in graphene

Exotic properties of a TMD monolayer

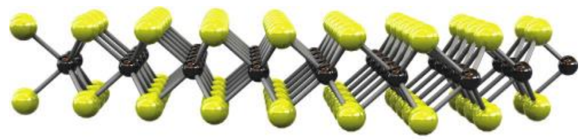

- ✓ Strong SOC
- ✓ Breaking inversion symmetry

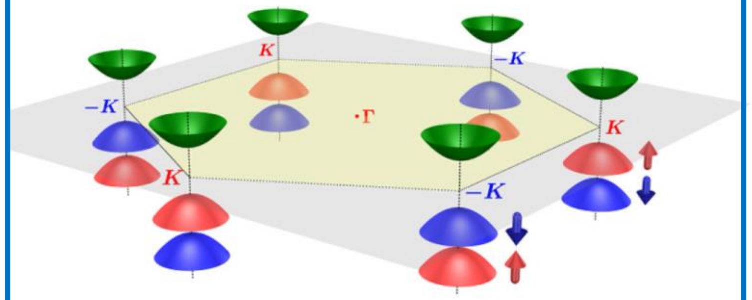

Giant spin splitting — ~150 meV MoS_2, ~460 meV WSe_2

Spin-valley locking

D. Xiao et al. , Phys. Rev. Lett. **108**, 196802 (2012)

Imprinted in graphene by proximity

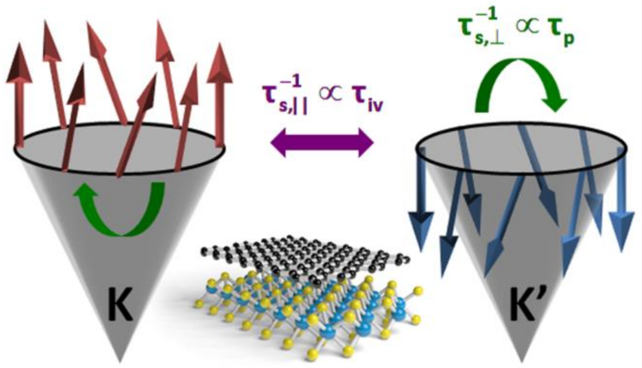

M. Gmitra et al. , Phys. Rev. B **93**, 155104 (2016)
J. H. Garcia et al. , Chem. Soc. Rev. **47**, 3359 (2018)

- ➢ WEAK ANTILOCALIZATION

Z. Wang *et al.*, Nature Comms. **6**, 8339 (2015)
B. Yang *et al.*, 2D Mater. **3**, 031012 (2016)
T. Wakamura *et al.*, Phys. Rev. Lett. **120**, 106802 (2018)
S. Zihlmann *et al.*, Phys. Rev. B **97**, 075434 (2018)

- ➢ ANISOTROPIC SPIN RELAXATION

T. S. Ghiasi *et al.*, Nano Lett. **17**, 7528 (2017)
L. A. Benitez *et al.*, Nature Phys. **14**, 303 (2018)

- ➢ SPIN HALL EFFECT

C. K. Safeer *et al.*, Nano Lett. **19**, 1074 (2019)
L. A. Benitez *et al.*, Nature Mater. **19**, 170 (2020)

- ➢ RASHBA-EDELSTEIN EFFECT

T. S. Ghiasi *et al.*, Nano Lett. **19,** 8758 (2019)
L. A. Benitez *et al.*, Nature Mater. **19,** 170 (2020)

SPIN HALL EFFECT: proximitized graphene

- SPIN HALL EFFECT induced by valley-Zeeman coupling?

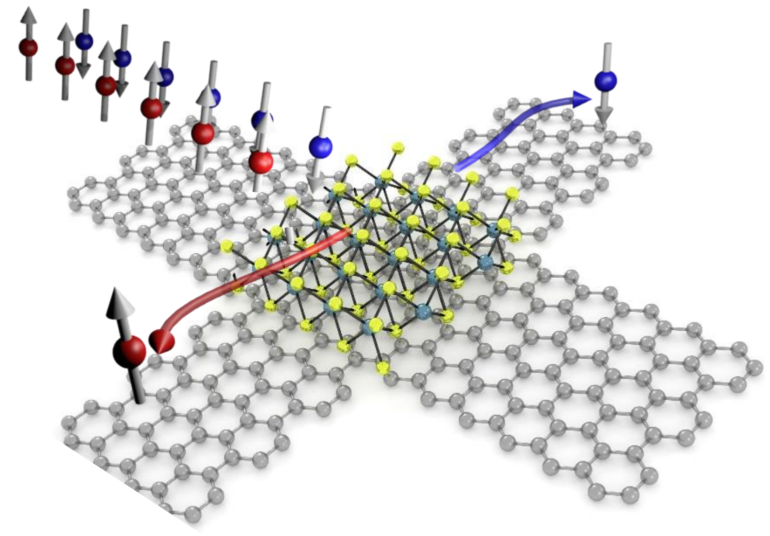

Theoretically predicted in absence of intervalley scattering:

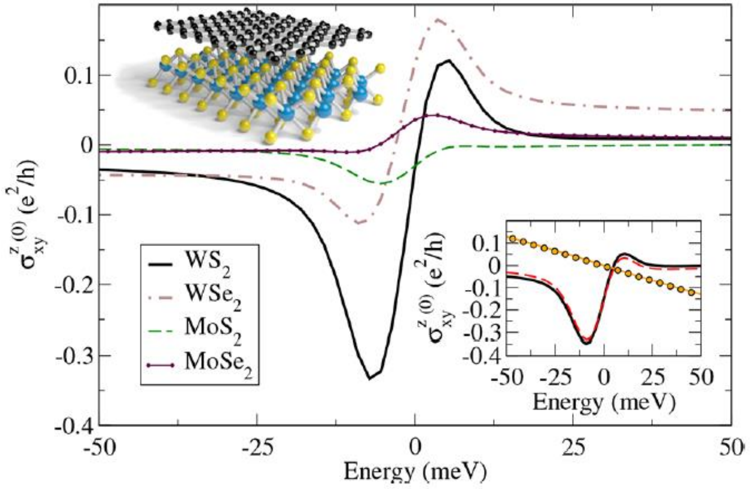

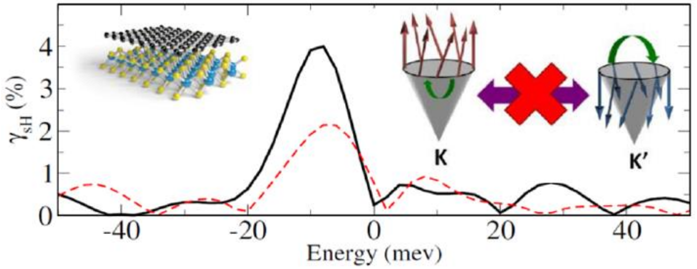

J. H. Garcia *et al.*, Nano Lett. **17**, 5078 (2017)

SPIN HALL EFFECT: proximitized graphene

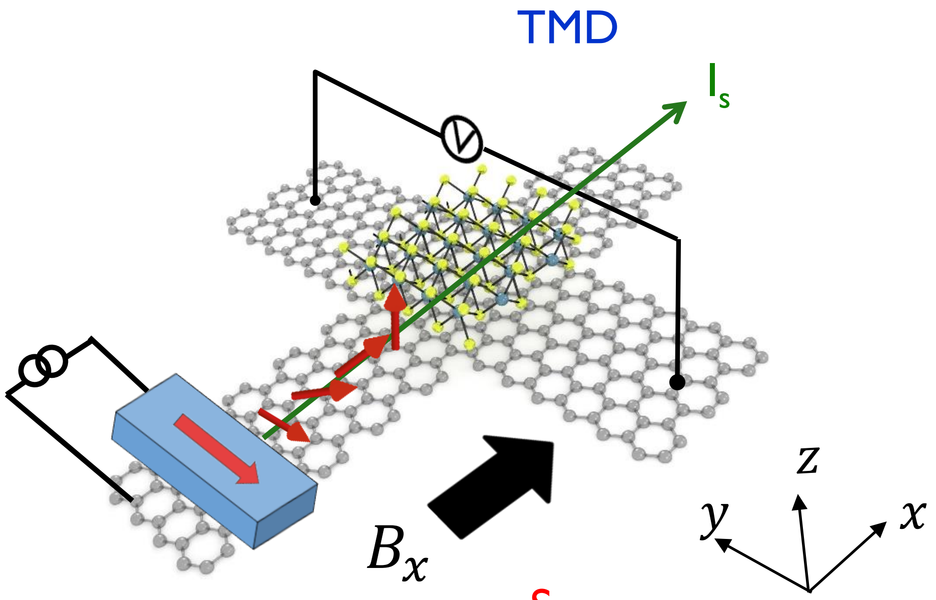

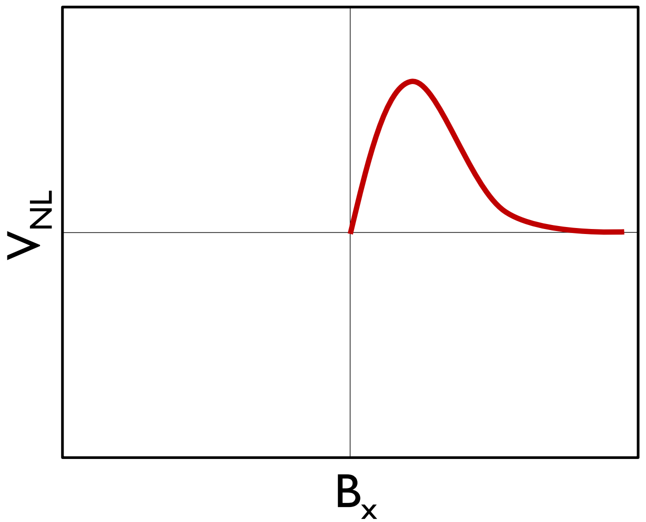

Precession = $s \times B_x$

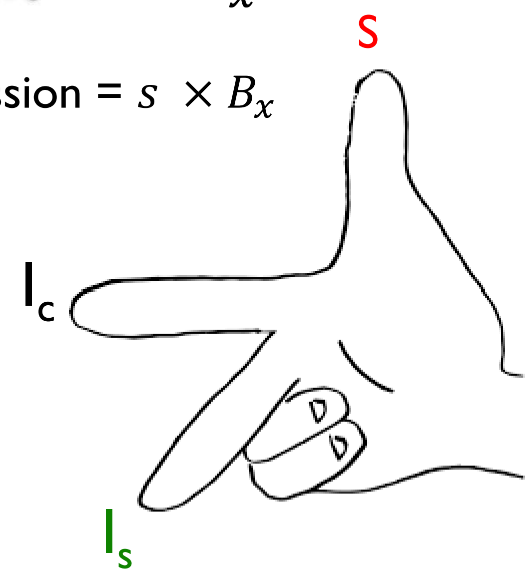

✓ Out-of-plane spins

C. K. Safeer, FC *et al.*, Nano Lett. **19**, 1074 (2019)

SPIN HALL EFFECT: proximitized graphene

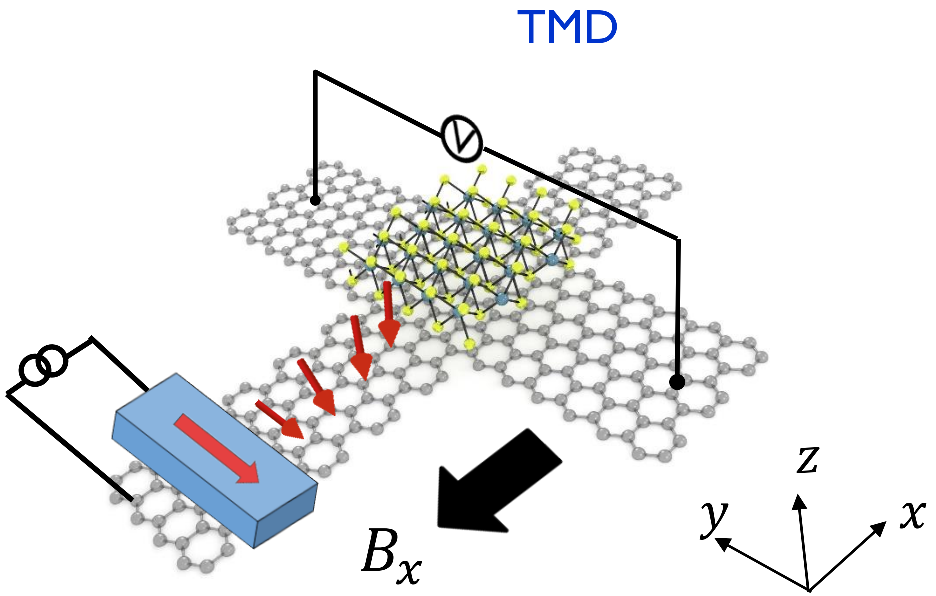

Precession = $s \times -B_x$

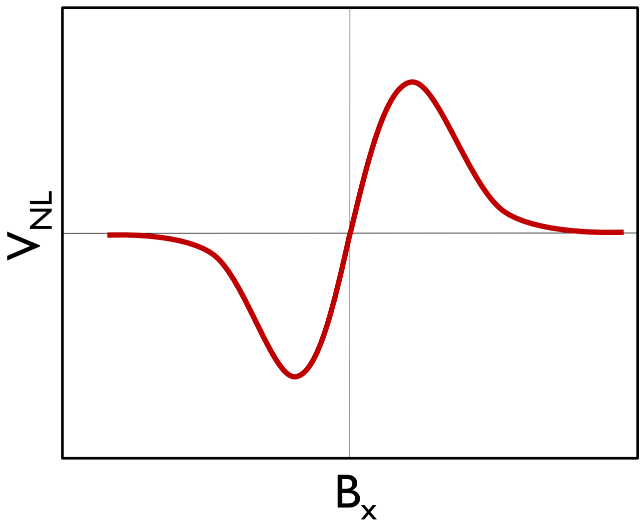

C. K. Safeer, FC *et al.*, Nano Lett. **19**, 1074 (2019)

SPIN HALL EFFECT: proximitized graphene

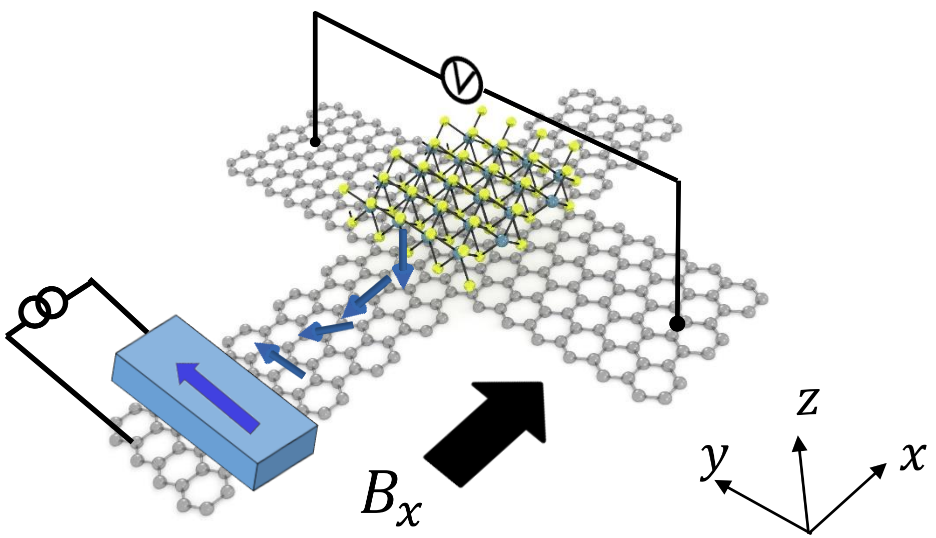

Precession = $-s \times B_x$

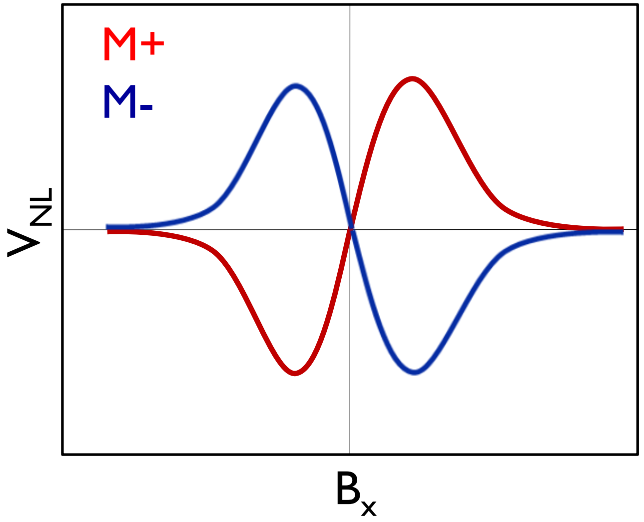

C. K. Safeer, FC *et al.*, Nano Lett. **19**, 1074 (2019)

SPIN HALL EFFECT: proximitized graphene

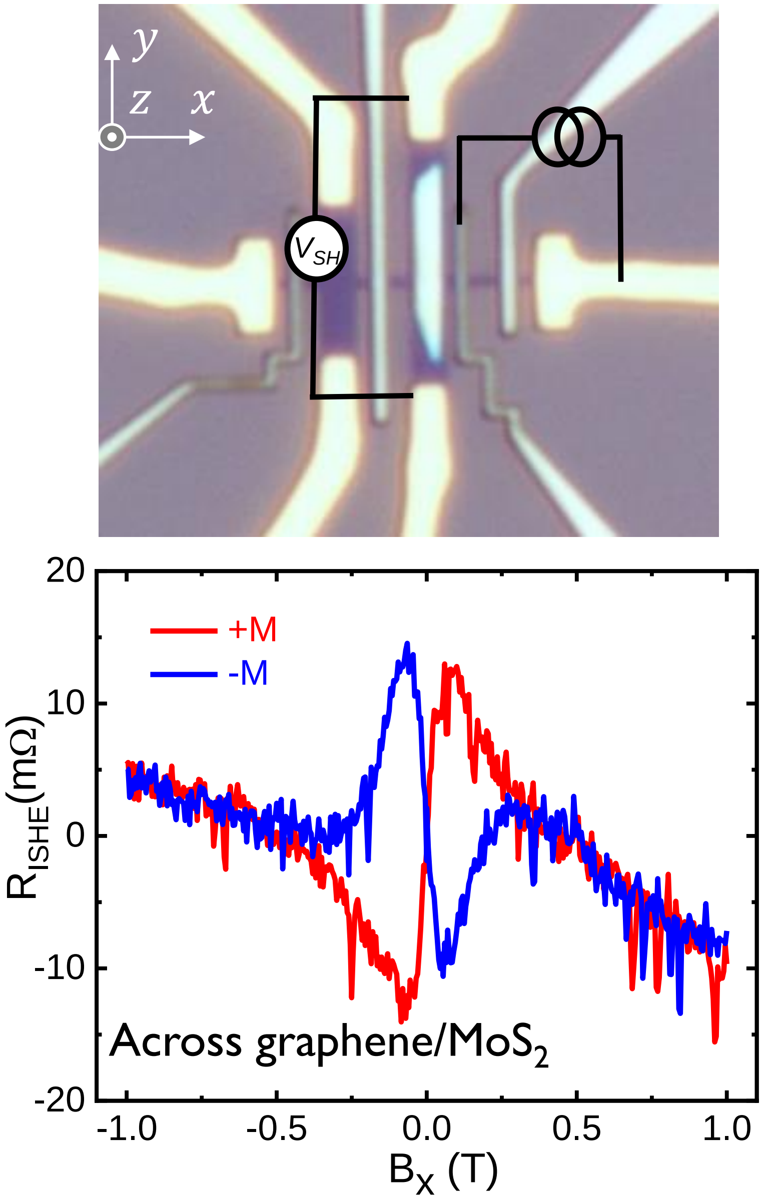

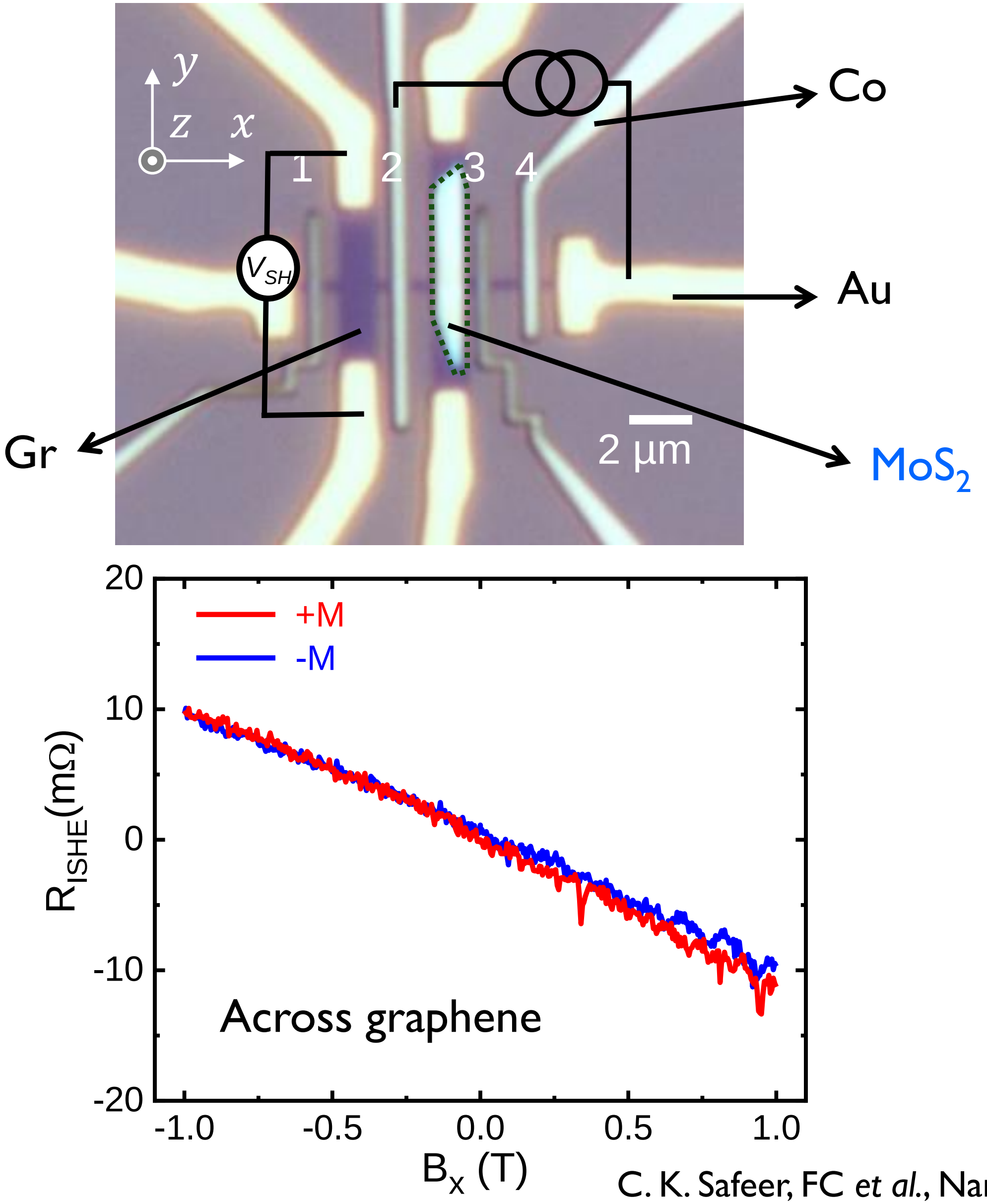

C. K. Safeer, FC *et al.*, Nano Lett. **19**, 1074 (2019)

SPIN HALL EFFECT: proximitized graphene

graphene/MoS_2

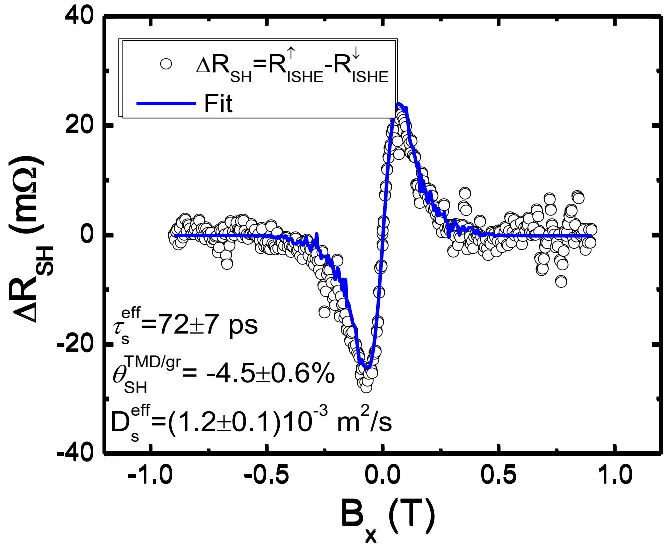

Spin Hall effect in graphene/MoS_2:

$\theta_{SH}^{TMD/gr}$ = –4.5 ± 0.6%

$\lambda_{TMD/gr}^{eff}$ = 300 ± 30 nm

$\theta_{SH}^{TMD/gr}\lambda_{TMD/gr}^{eff}$ = 13.5 nm at 10 K

= 1.4 nm at 300 K

- Combination of long spin transport and large SHE in the same material

C. K. Safeer, FC *et al.*, Nano Lett. **19**, 1074 (2019)

graphene/WSe_2

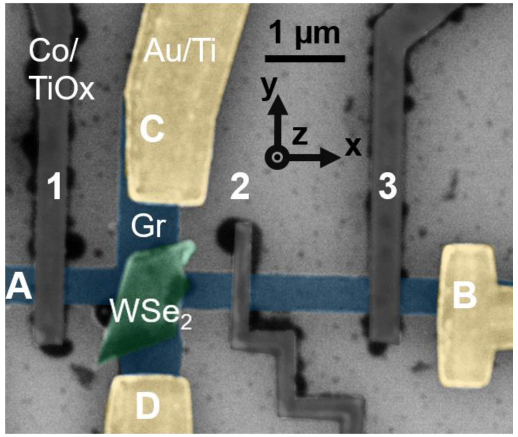

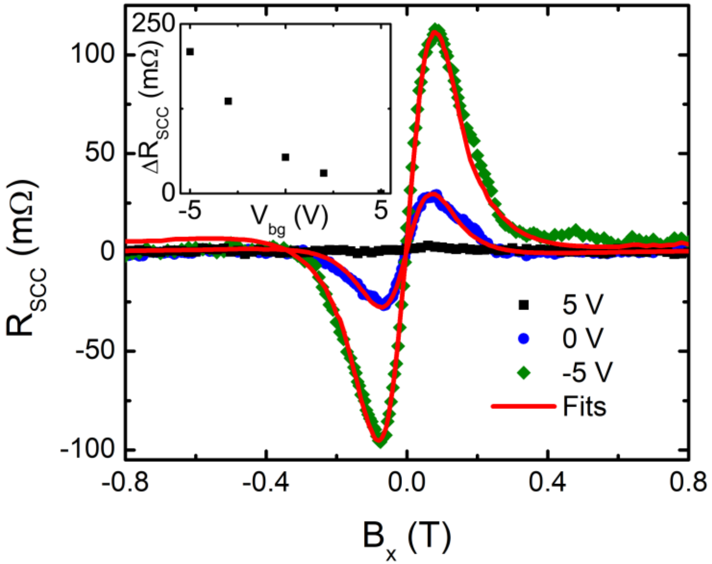

$\theta_{SH}^{TMD/gr}\lambda_{TMD/gr}^{eff}$ = 40 nm at 100 K and -5 V

- Gate tunability of the SHE
- Largest efficiency reported

F. Herling, FC *et al.*, APL Mater. **8**, 071103 (2020)

RASHBA-EDELSTEIN EFFECT: reminder

✓ Systems (typically 2D) with broken inversion symmetry

Direct effect **(REE)**

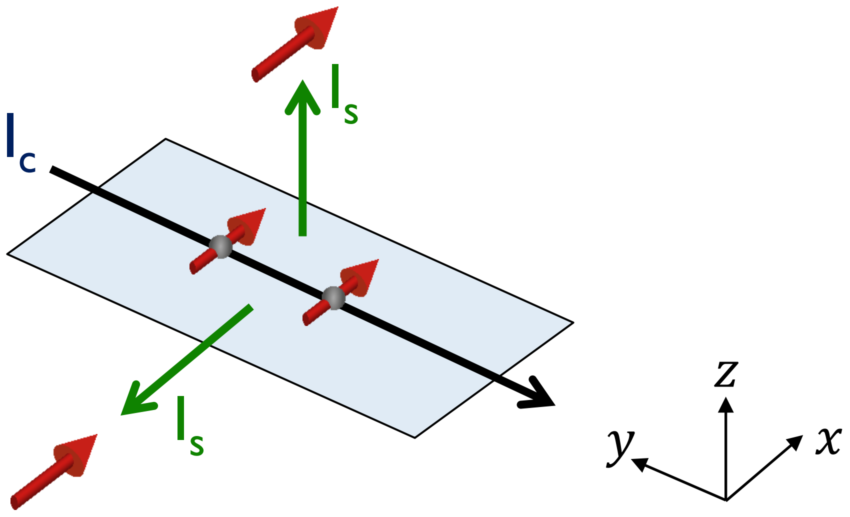

Spin current generation

Inverse effect **(IREE)**

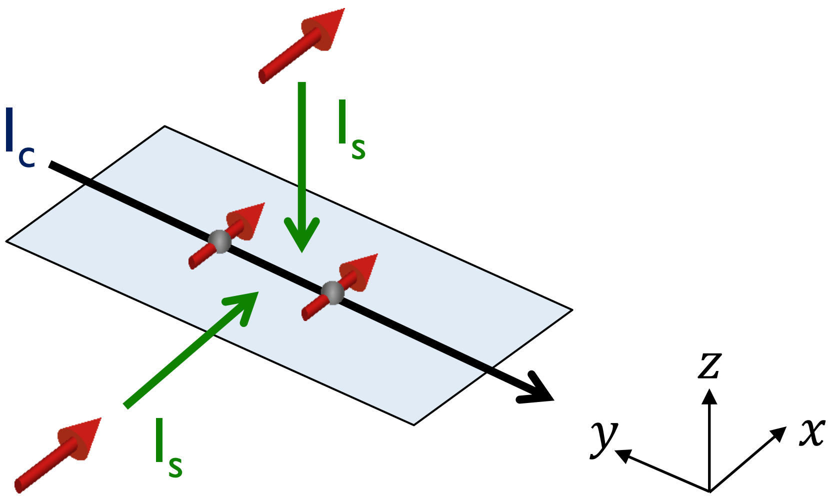

$$\boxed{\lambda_{IEE} = \frac{j_c(2D)}{j_s(3D)}} \quad [L]$$

$$\boxed{\alpha_{IEE} = \frac{j_c(2D)}{j_s(2D)}}$$

Spin current detection

RASHBA-EDELSTEIN EFFECT: proximitized graphene

➢ RASHBA-EDELSTEIN EFFECT induced by Rashba coupling?

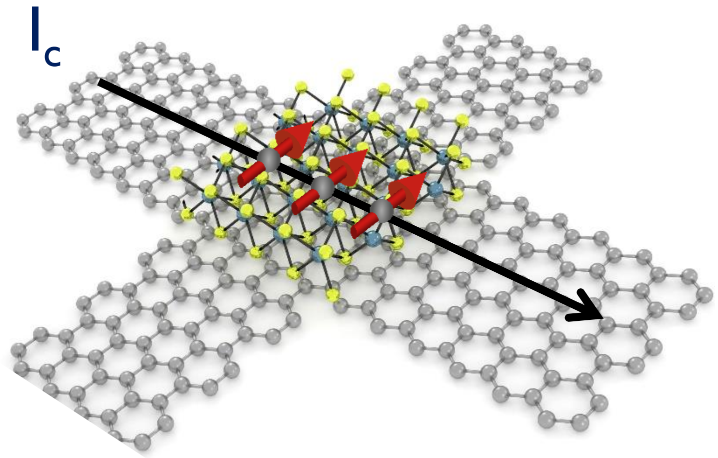

Theoretically predicted:

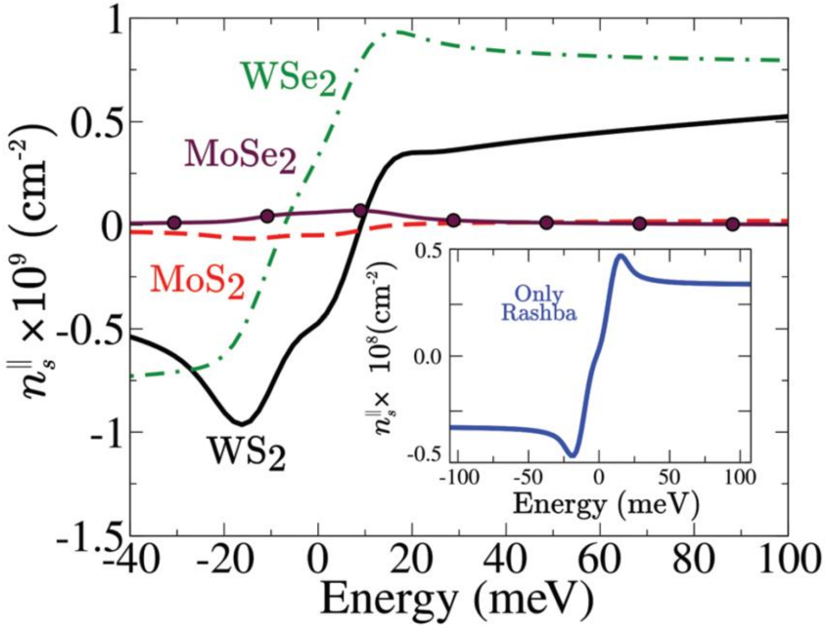

Experimentally observed:

T. S. Ghiasi *et al.*, Nano Lett. **19,** 8758 (2019)
L. A. Benitez *et al.*, Nature Mater. **19,** 170 (2020)

M. Offidani et al., Phys. Rev. Lett. **119**, 196801 (2017)
J. H. Garcia et al., Chem. Soc. Rev. **47**, 3359 (2018)

SPIN-TO-CHARGE CONVERSION in twisted graphene/WSe_2

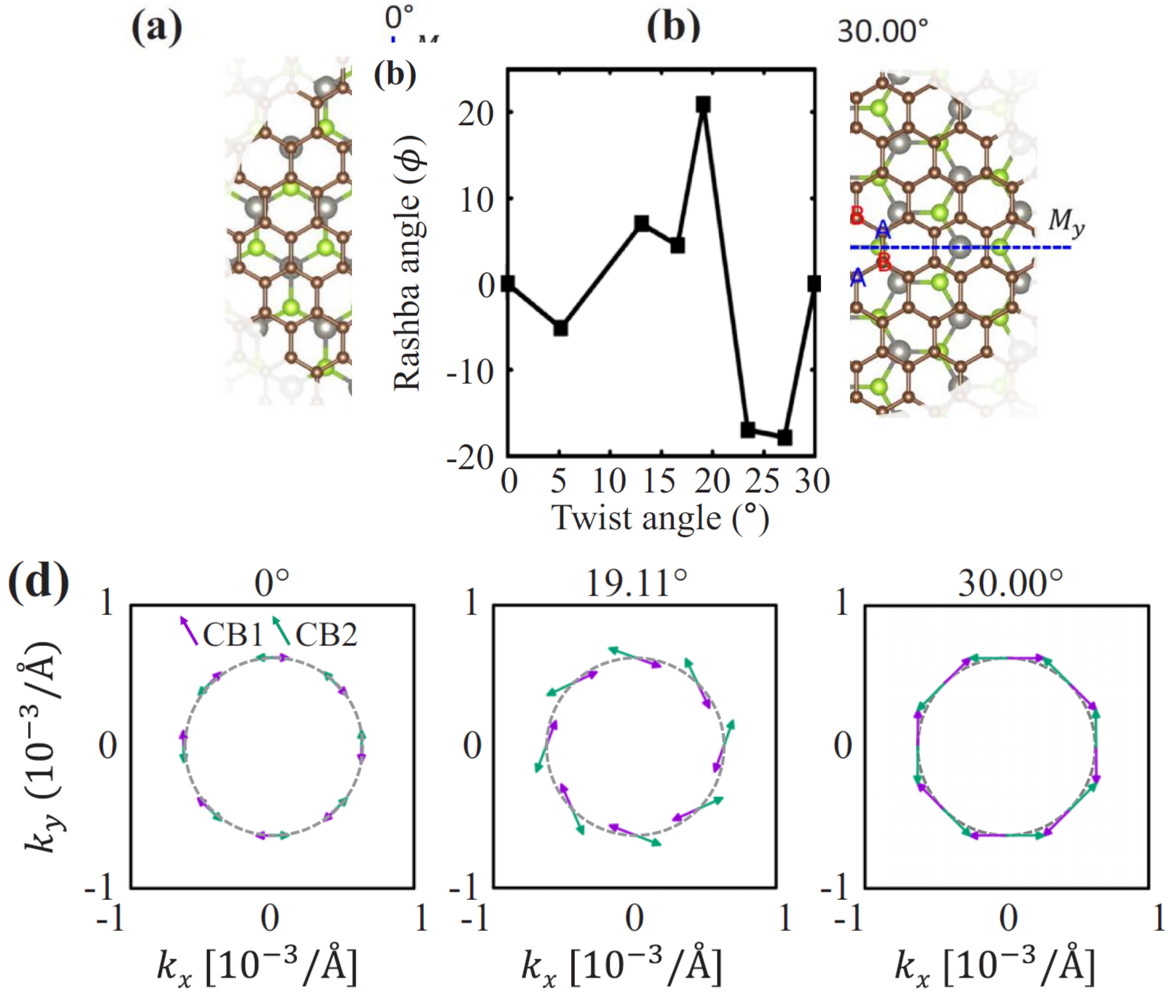

Theoretical calculation in twisted Gr/WSe_2 heterostructures:

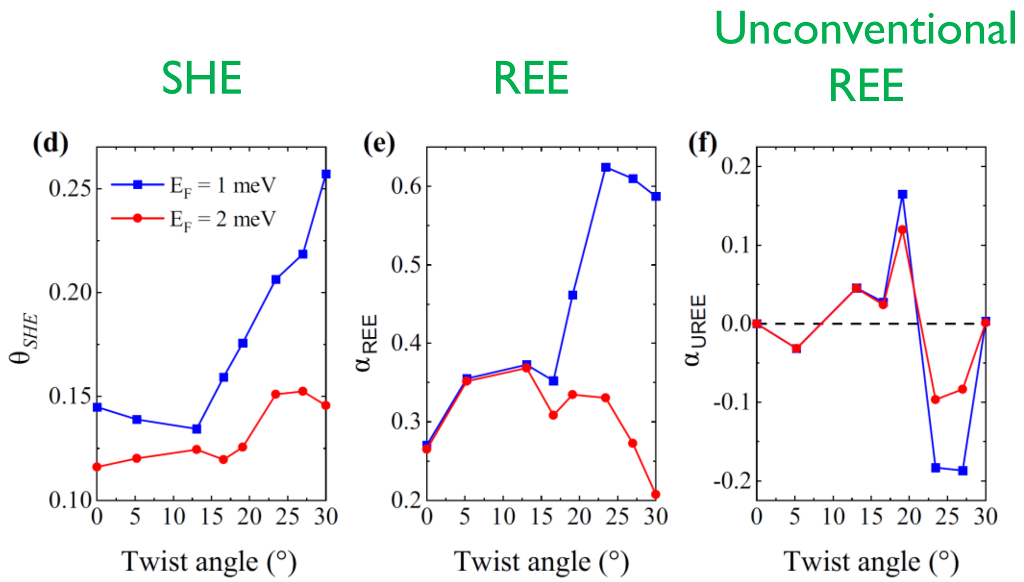

Spins out of plane
Z spins

Spins in plane
Perp. to current
X spins

Spins in plane
Paral. to current
Y spins

Lee *et al.*, Phys, Rev. B **106**, 165420 (2022)

SPIN-TO-CHARGE CONVERSION: z-spins

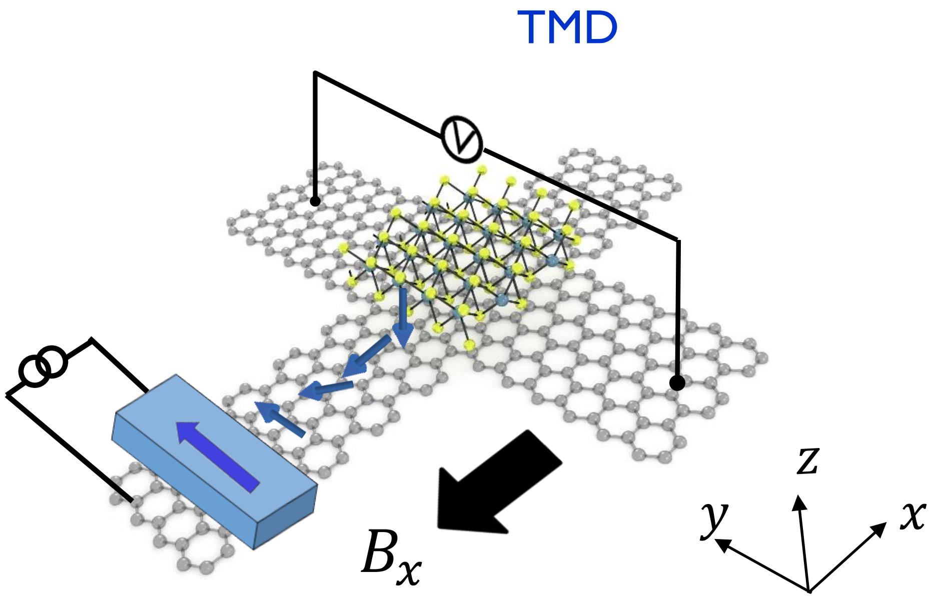

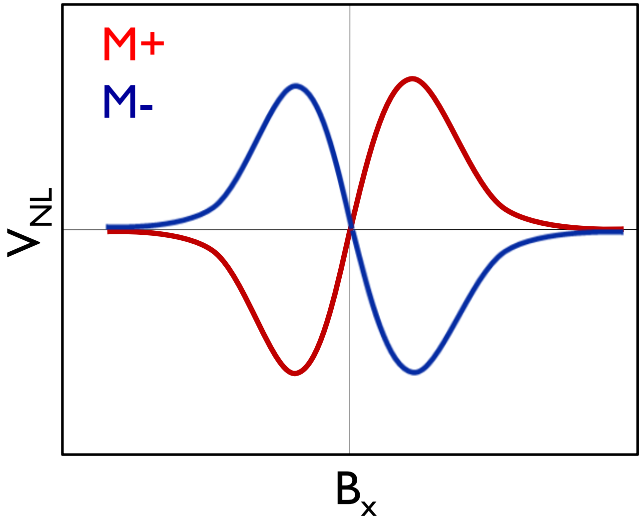

Precession = $-s \times B_x$

✓ SHE in proximitized graphene

SPIN-TO-CHARGE CONVERSION: x-spins

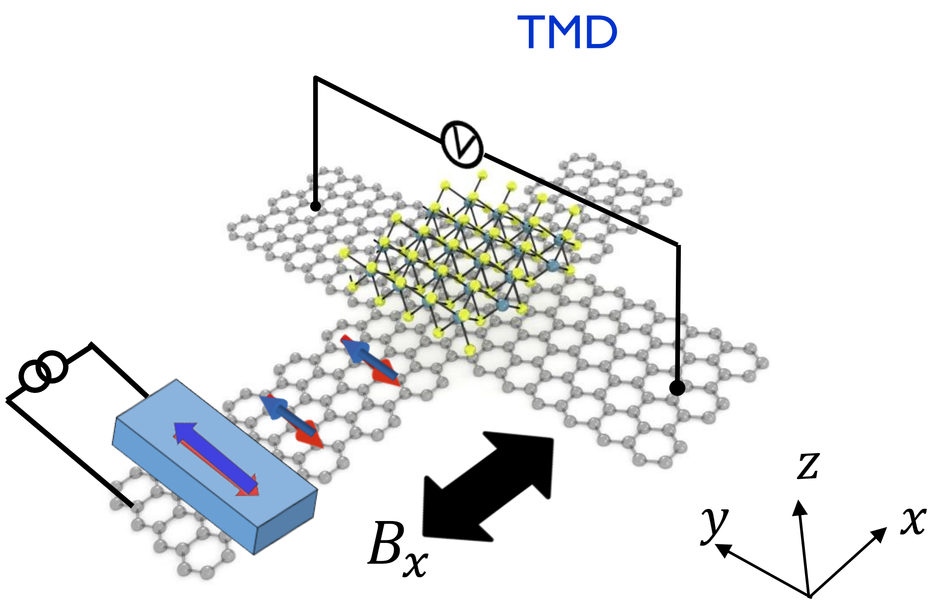

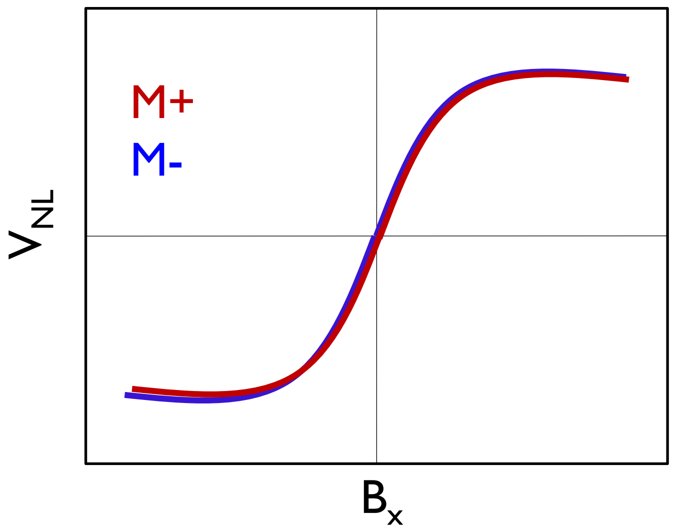

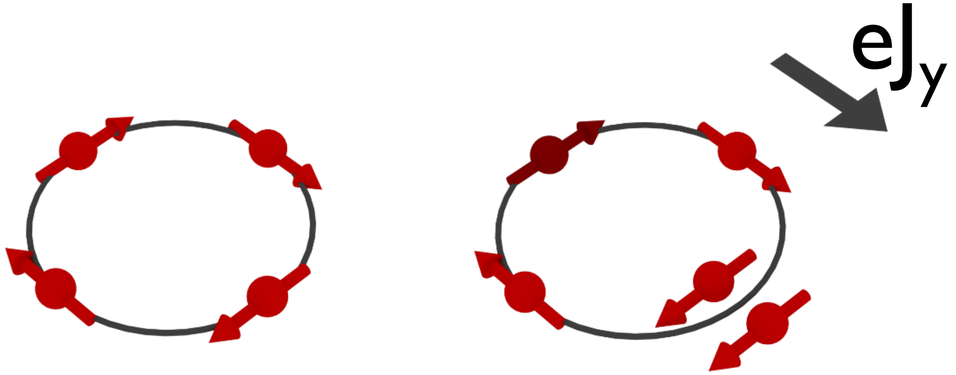

✓ REE in proximitized graphene

SPIN-TO-CHARGE CONVERSION: y-spins

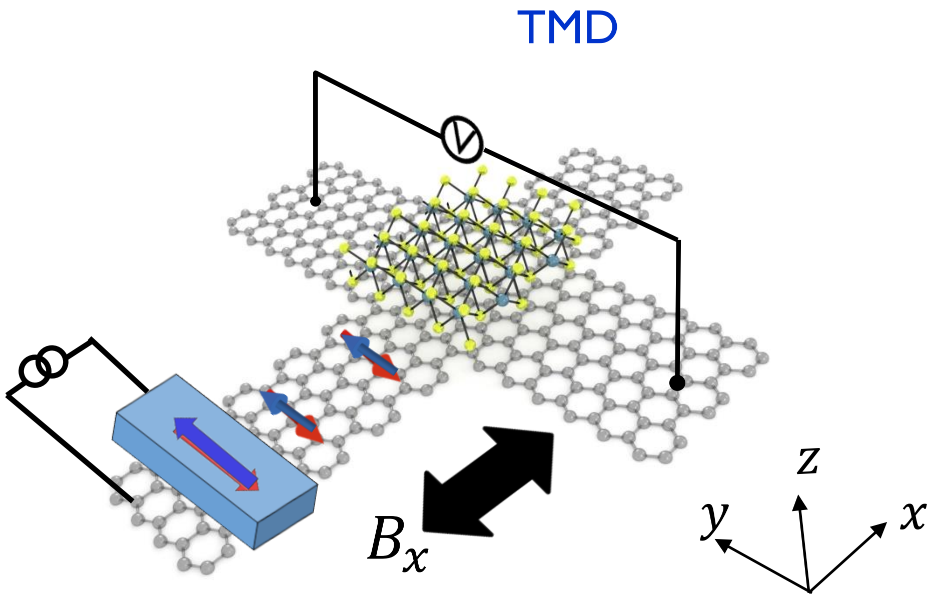

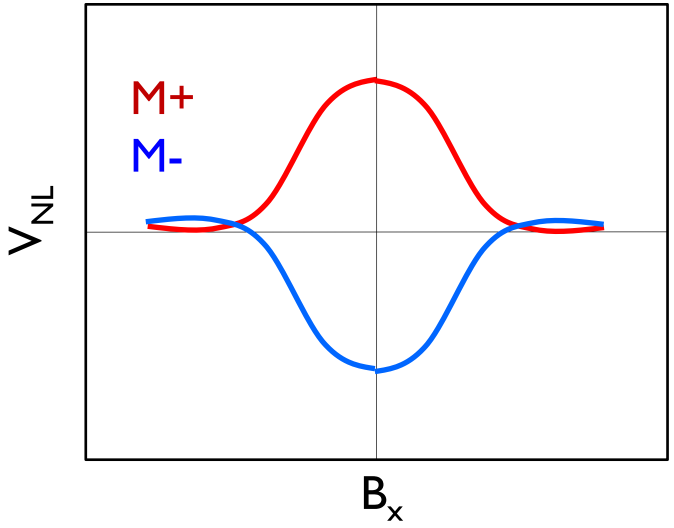

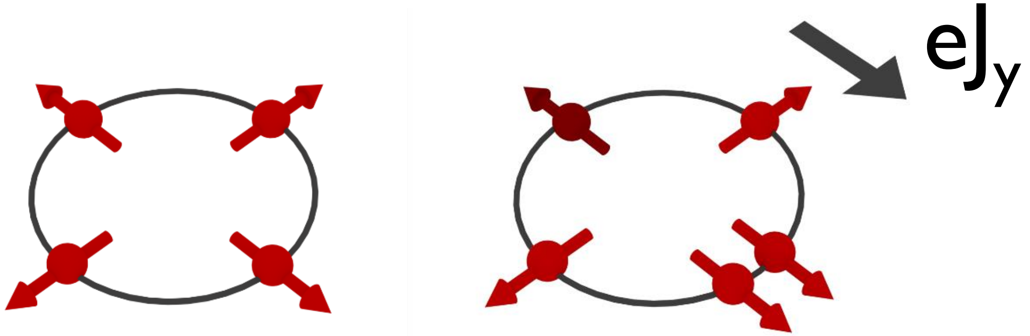

✓ Unconventional REE in proximitized graphene

SPIN-TO-CHARGE CONVERSION in twisted graphene/WSe_2

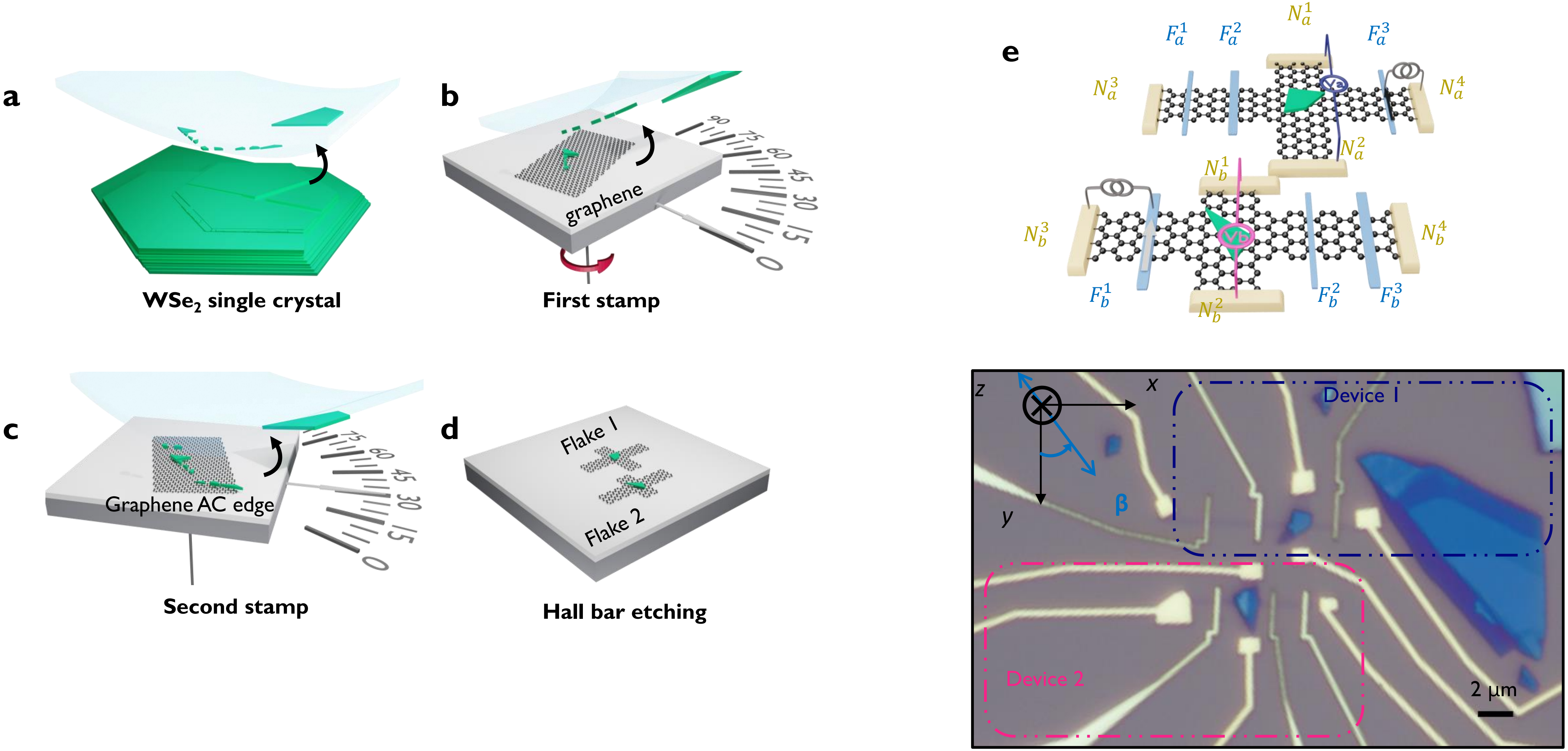

H. Yang, FC *et al.*, submitted

SPIN-TO-CHARGE CONVERSION in twisted graphene/WSe_2

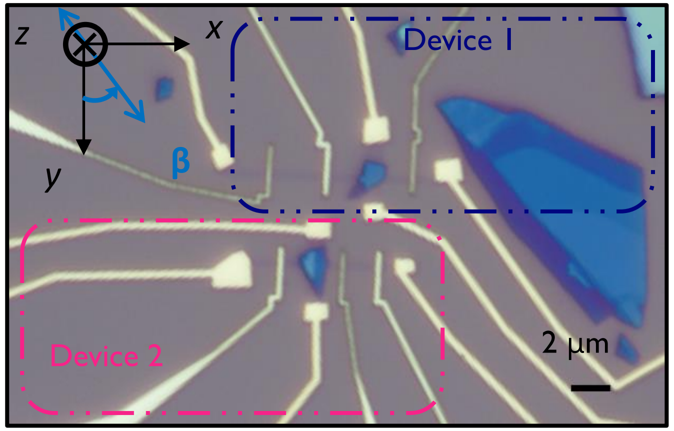

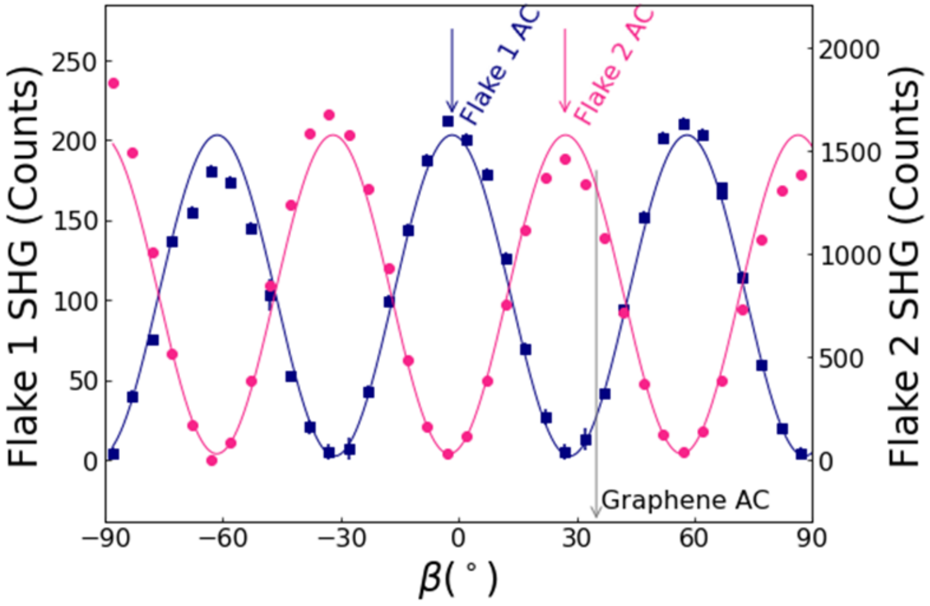

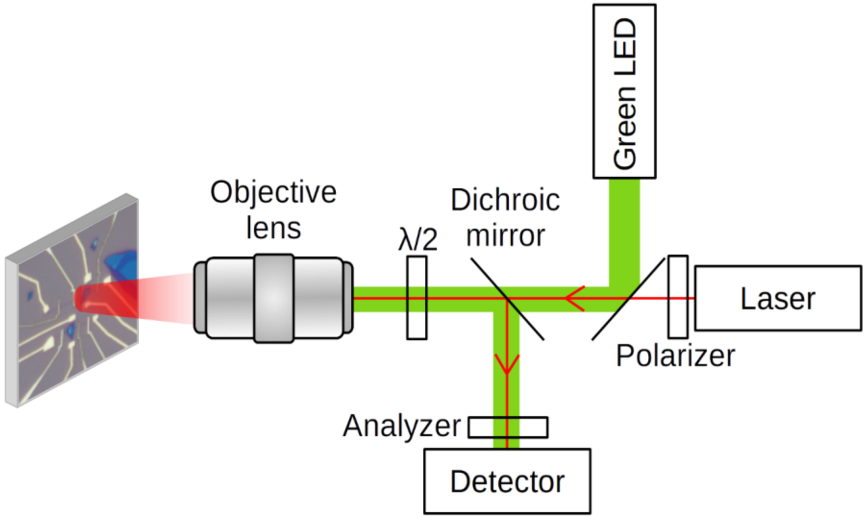

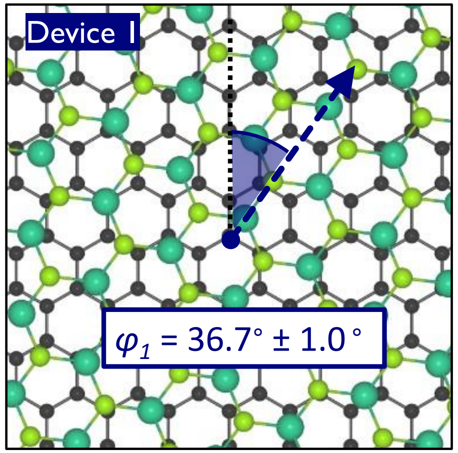

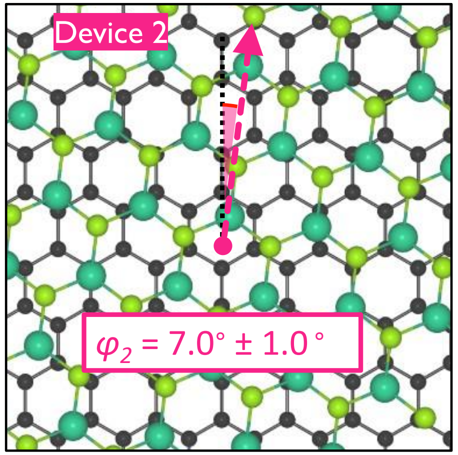

H. Yang, FC *et al.*, submitted

SPIN-TO-CHARGE CONVERSION in twisted graphene/WSe$_2$

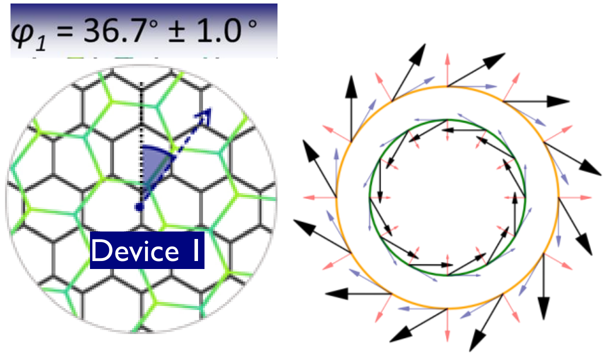

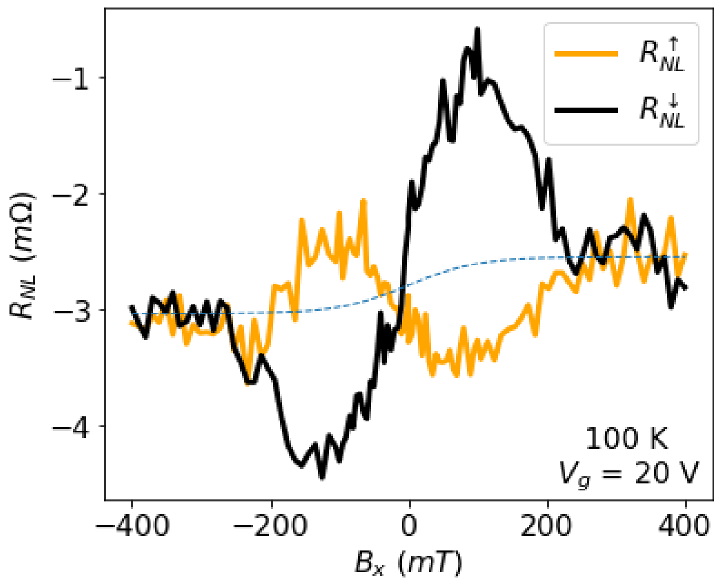

$$R_{SCC} = \frac{R_{NL}^{\uparrow} - R_{NL}^{\downarrow}}{2}$$

antisym

sym

$$R_{avg} = \frac{R_{NL}^{\uparrow} + R_{NL}^{\downarrow}}{2}$$

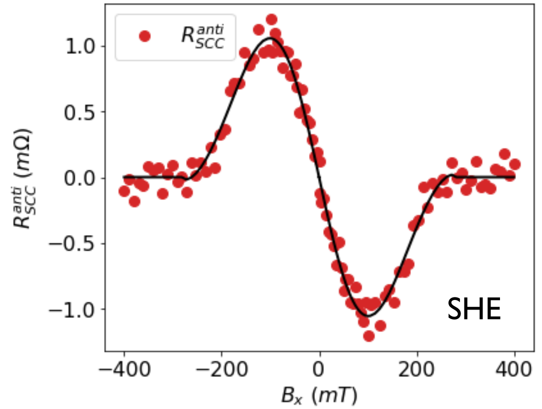

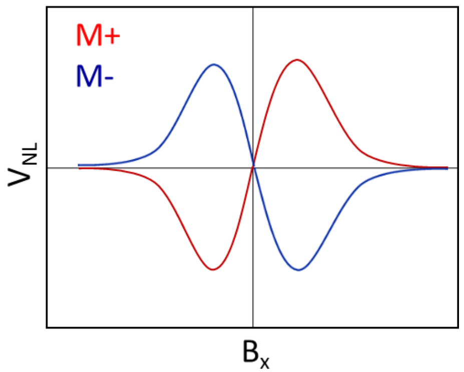

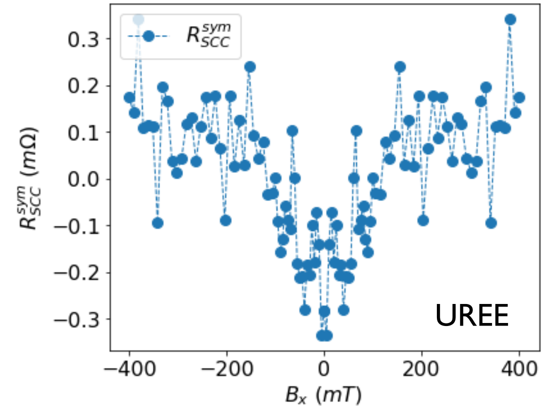

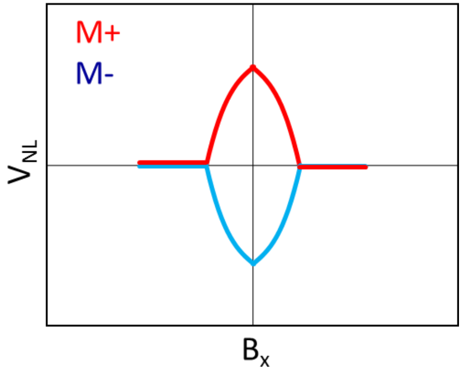

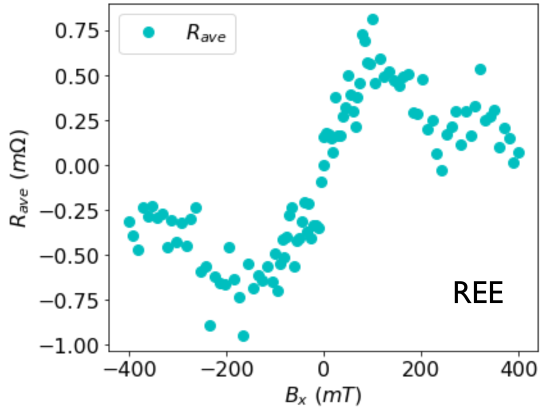

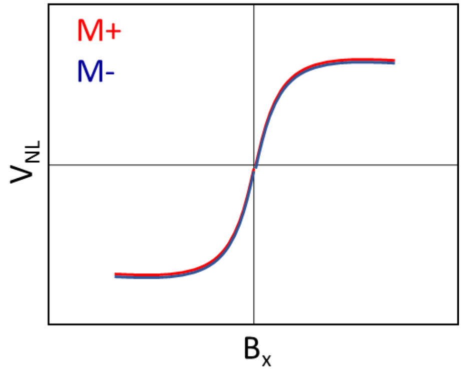

H. Yang, FC *et al.*, submitted

SPIN-TO-CHARGE CONVERSION in twisted graphene/WSe_2

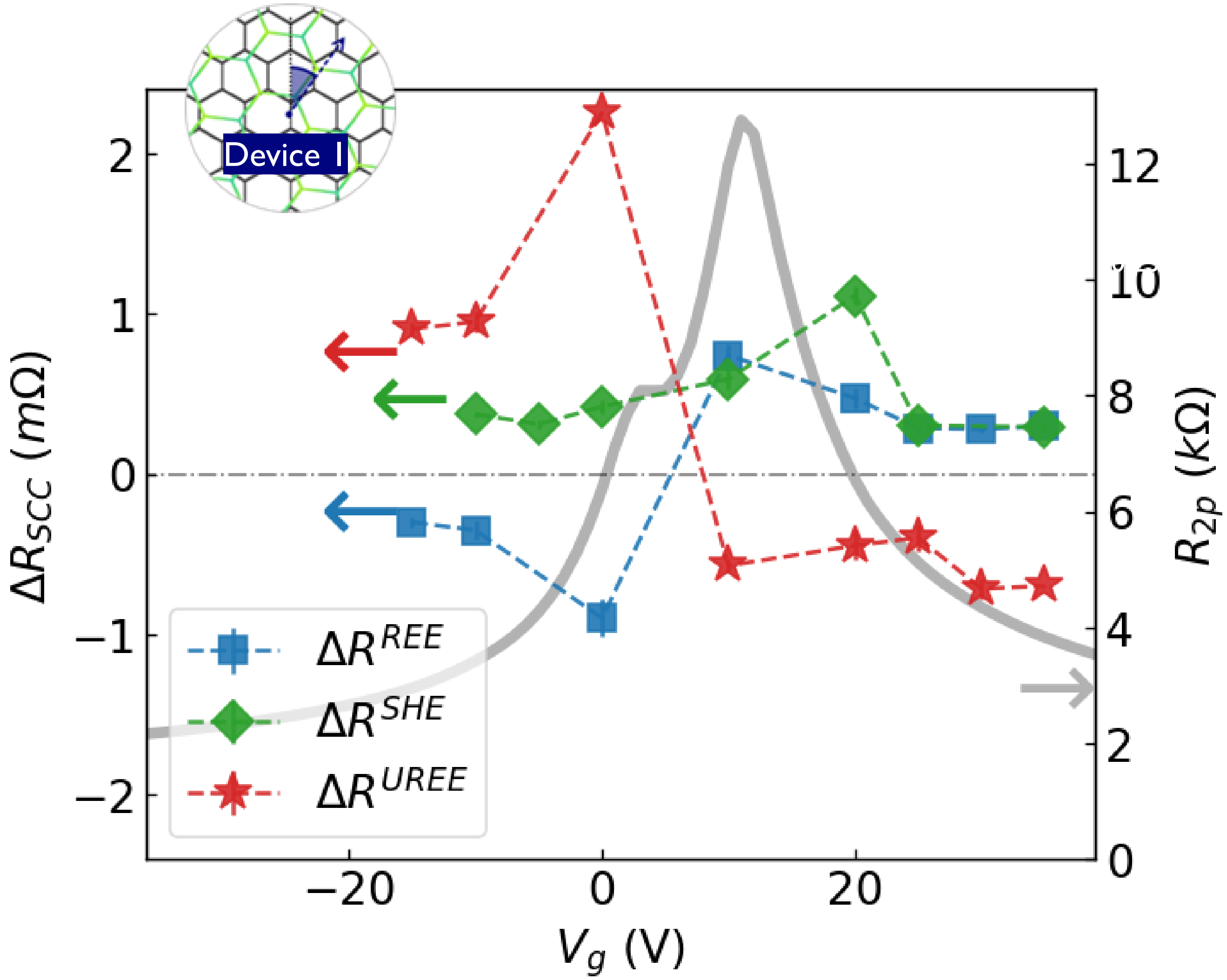

H. Yang, FC *et al.*, submitted

- All 3 signals are gate tunable
- Both REE and UREE signals change sign at CNP

SPIN-TO-CHARGE CONVERSION in twisted graphene/WSe_2

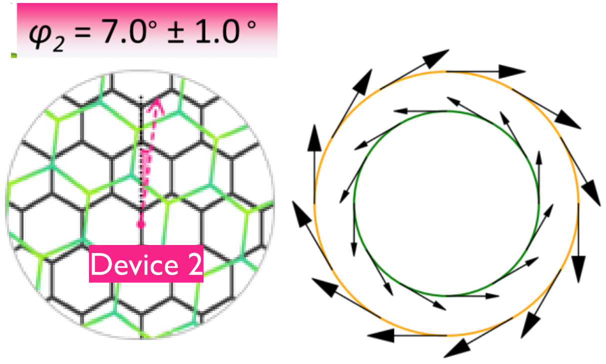

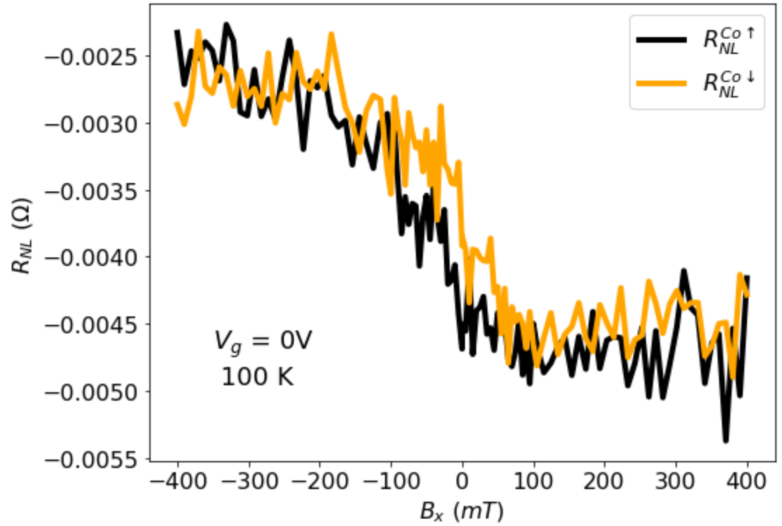

$$R_{SCC} = \frac{R_{NL}^{\uparrow} - R_{NL}^{\downarrow}}{2}$$

antisym

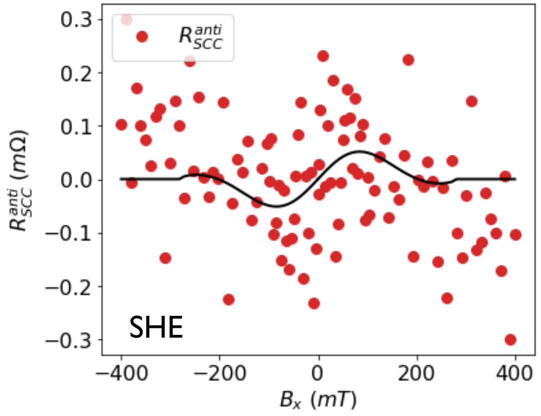

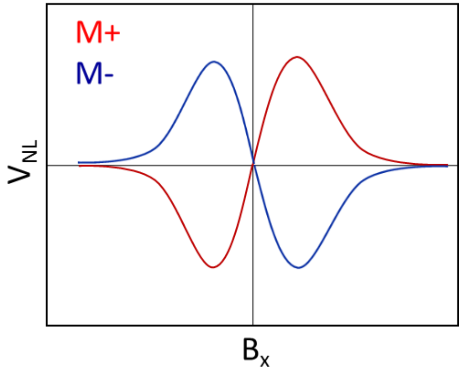

sym

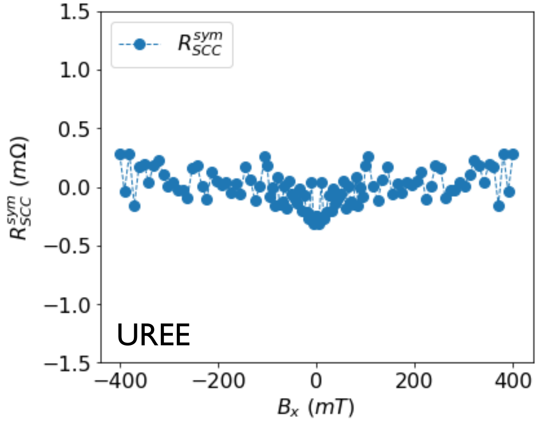

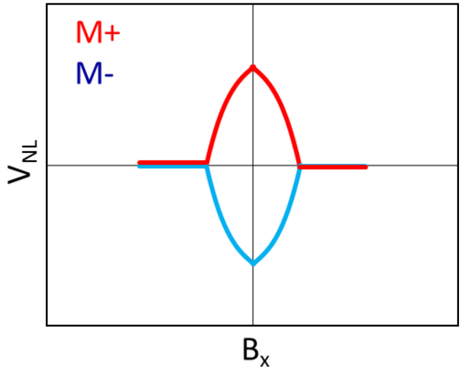

$$R_{avg} = \frac{R_{NL}^{\uparrow} + R_{NL}^{\downarrow}}{2}$$

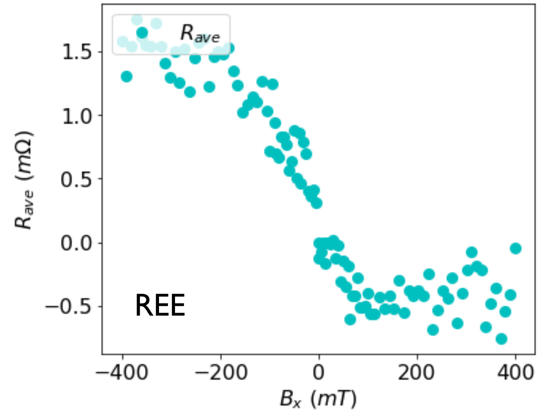

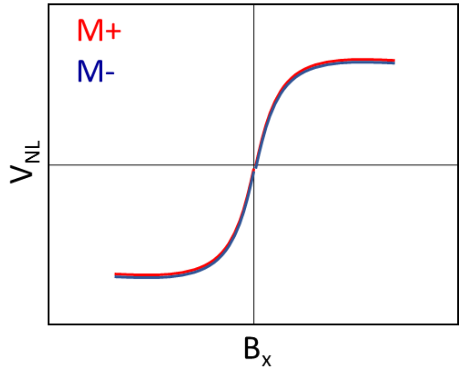

H. Yang, FC *et al.*, submitted

SPIN-TO-CHARGE CONVERSION in twisted graphene/WSe_2

Device 1

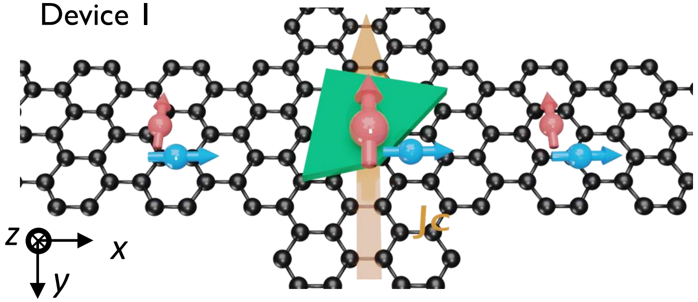

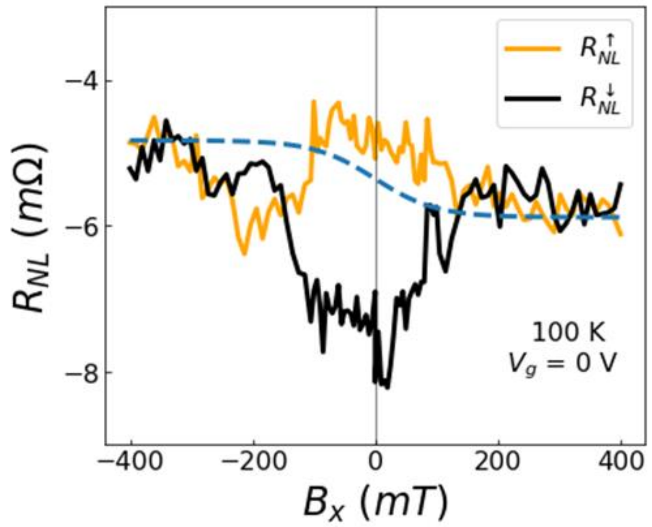

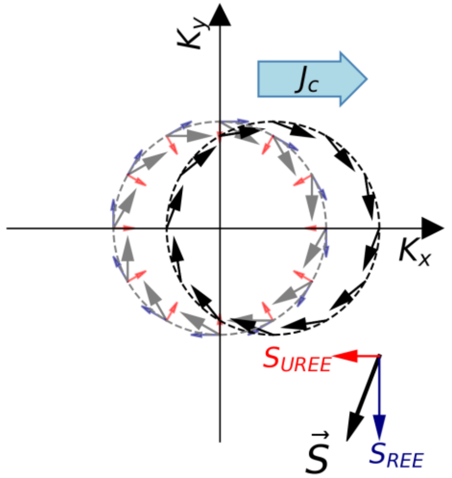

Device 3

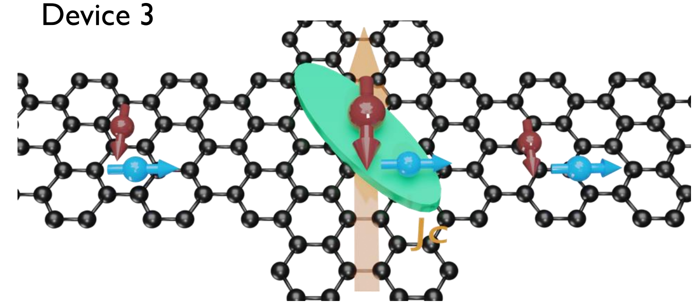

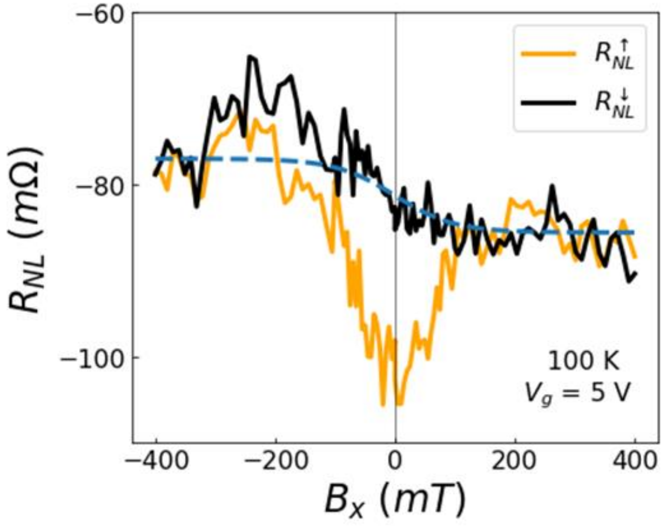

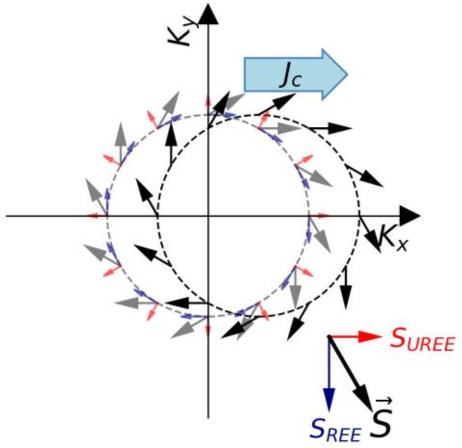

H. Yang, FC *et al.*, submitted

SPIN-TO-CHARGE CONVERSION in twisted graphene/WSe_2

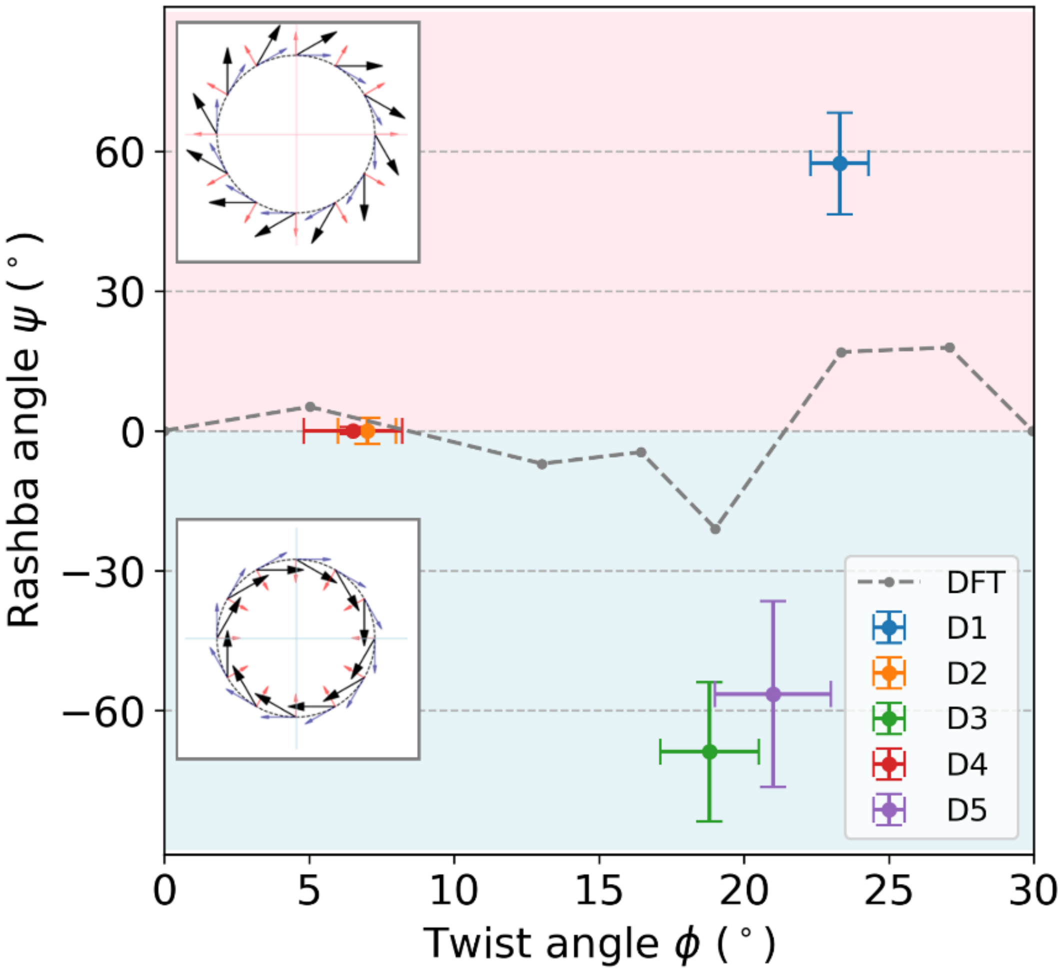

- Twist angle tunes Rashba angle
- Excellent agreement with theory

Theory: Lee *et al.*, Phys, Rev. B **106**, 165420 (2022)
Experiment: H. Yang, FC *et al.*, submitted

Chiral Tellurium crystals

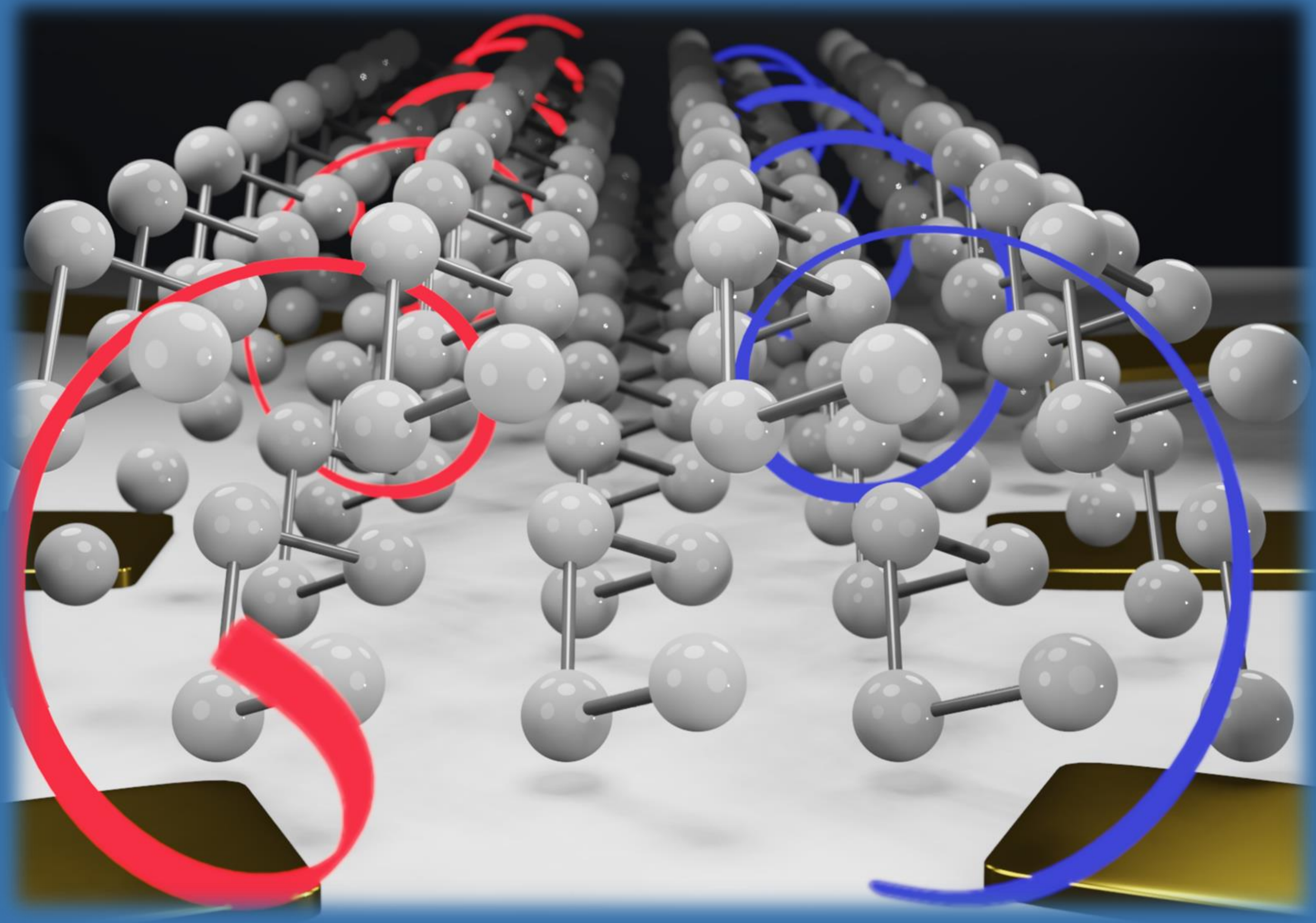

CHIRAL COMPOUNDS IN NATURE

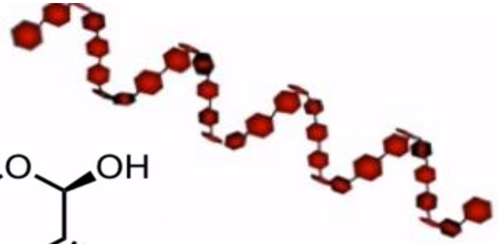

Sugar

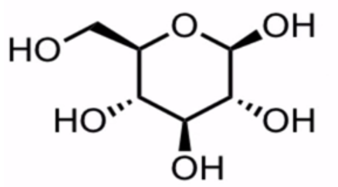

glucose

Proteins

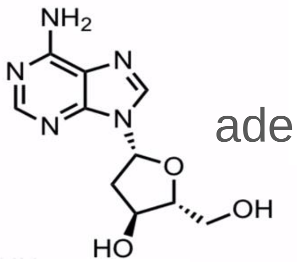

adenine

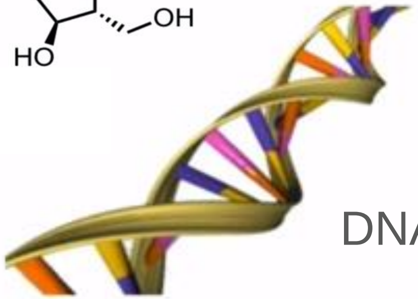

DNA

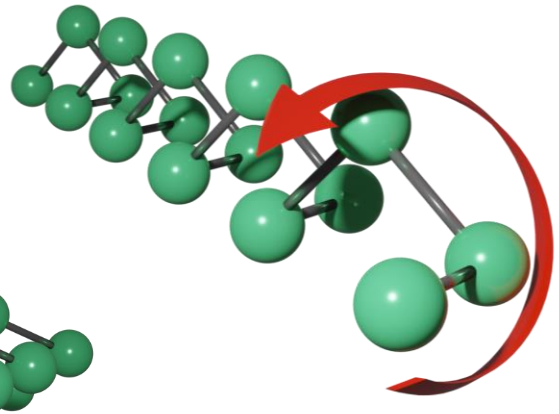

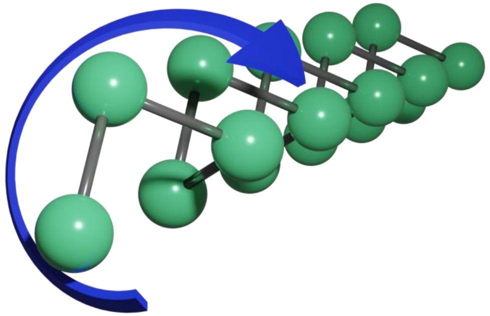

Trigonal Tellurium

TELLURIUM: fabrication of nanowires

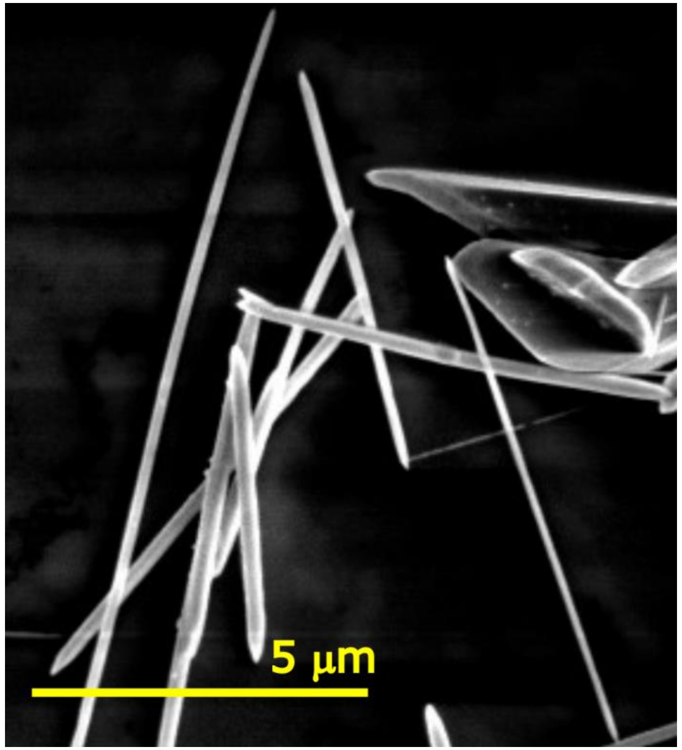

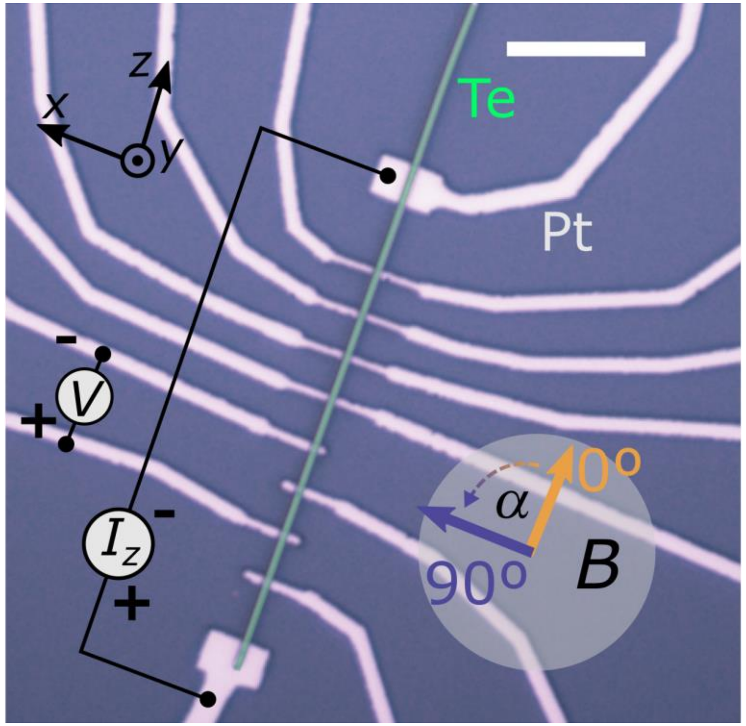

F. Calavalle *et al.*, Nat. Mater. **21**, 526 (2022)

TELLURIUM: structural characterization

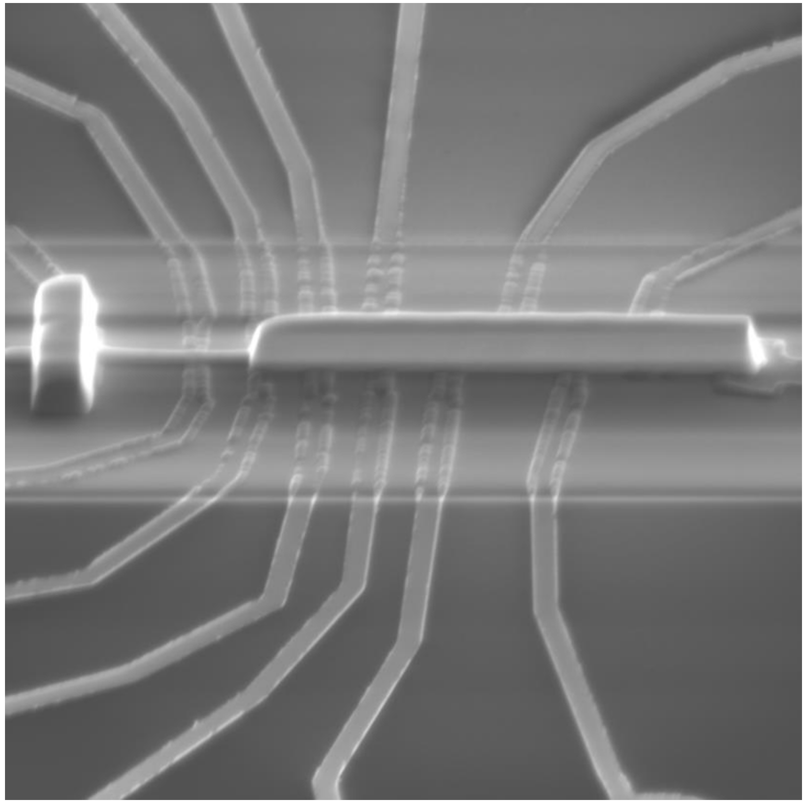

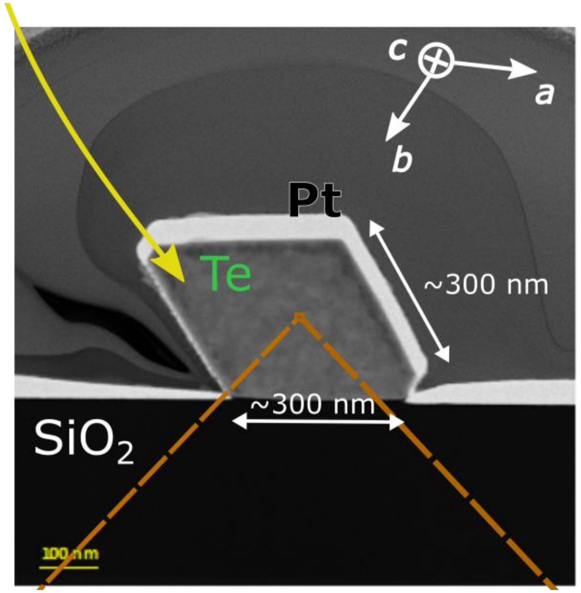

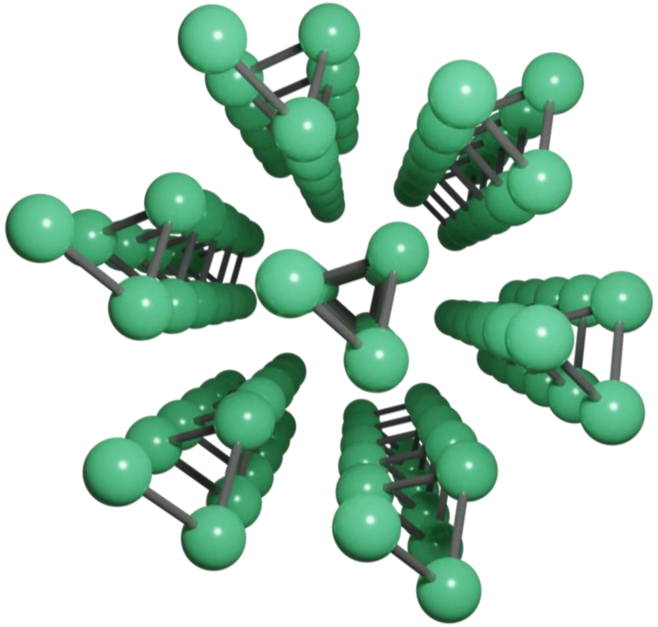

F. Calavalle *et al.*, Nat. Mater. **21**, 526 (2022)

TELLURIUM: handedness identification

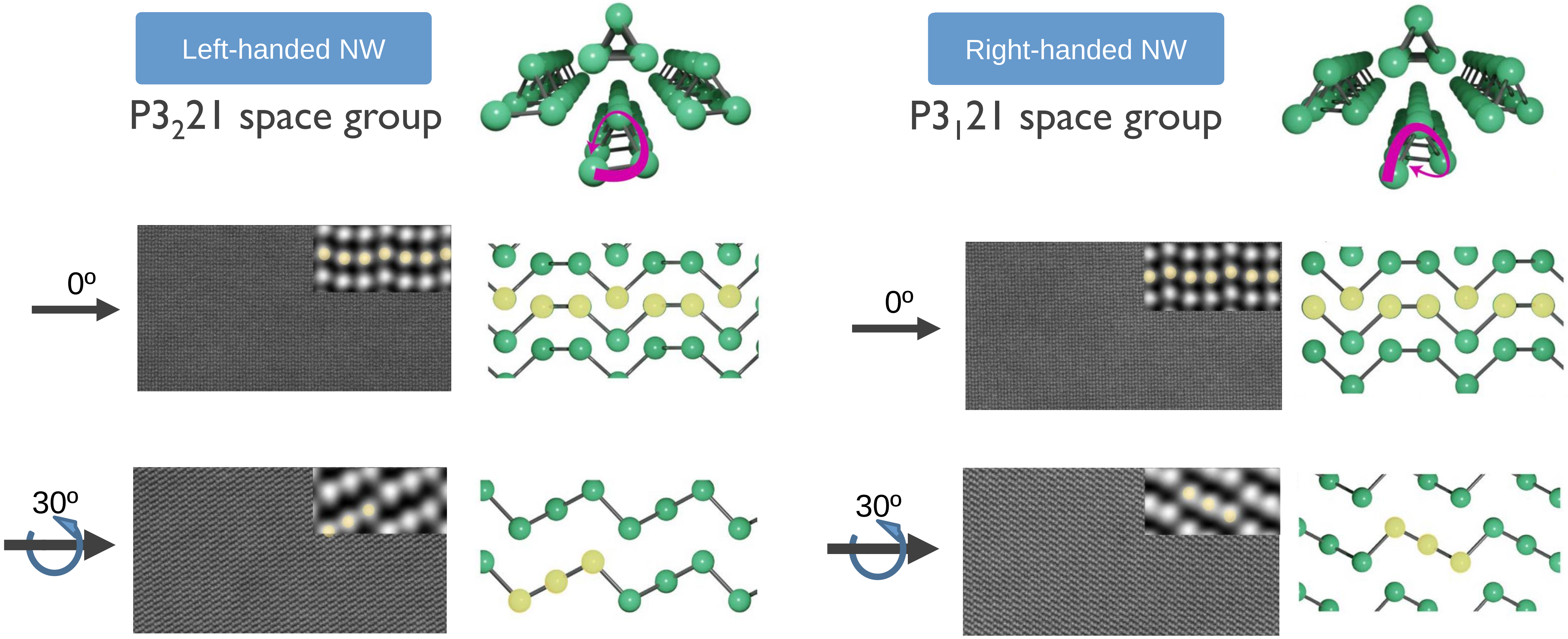

F. Calavalle *et al.*, Nat. Mater. **21**, 526 (2022)

TELLURIUM: spin texture

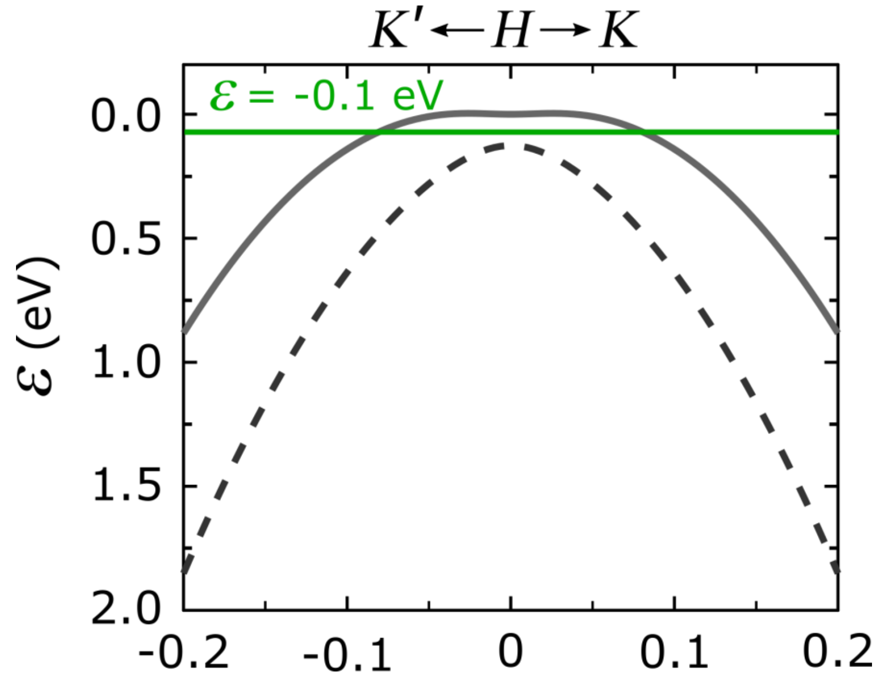

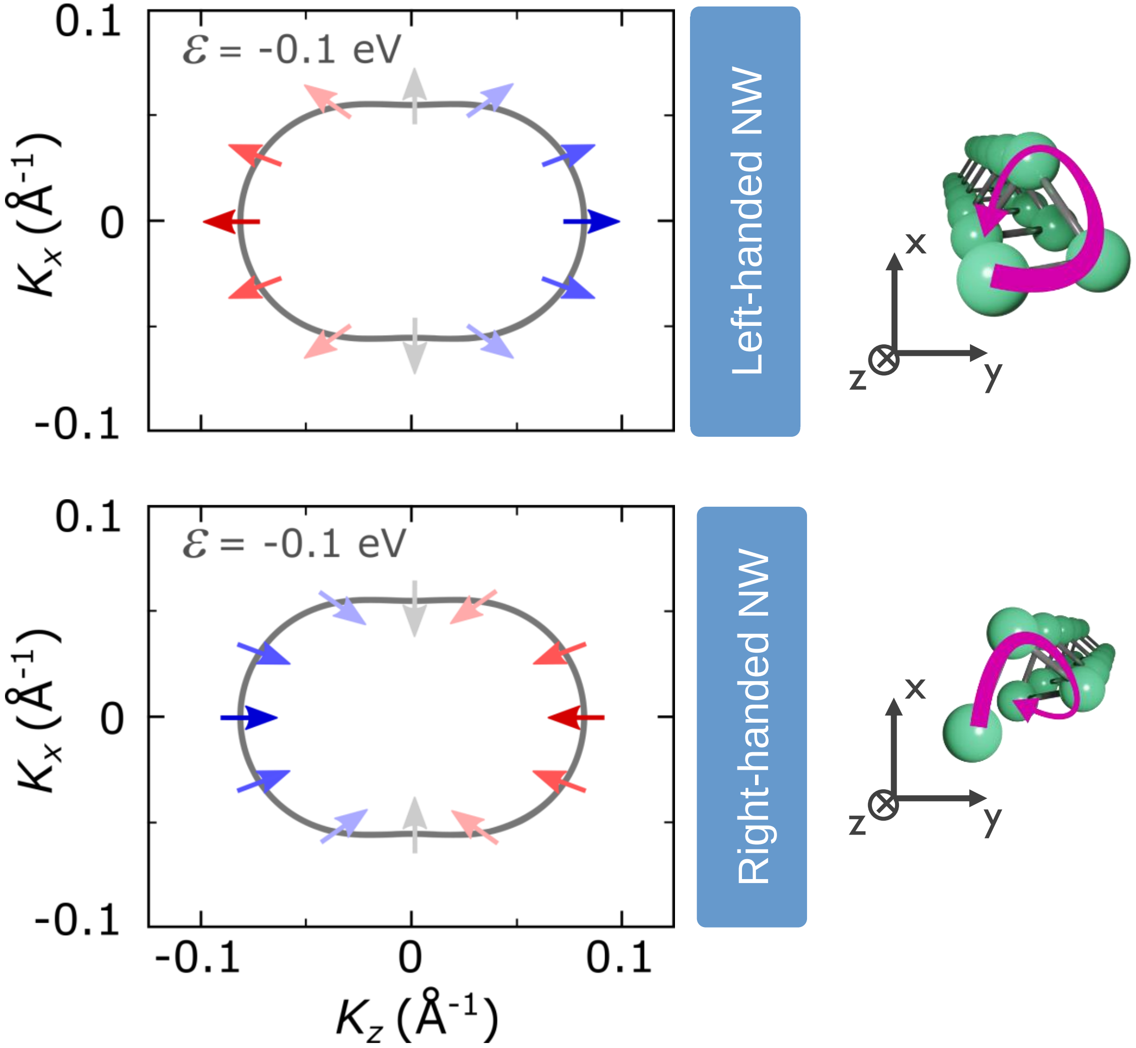

$$H(\mathbf{k}) = -\Delta - Ak_z^2 - B\sqrt{k_x^2 + k_y^2} + \chi\left[\frac{\Delta}{\sqrt{k_x^2 + k_y^2}}\left(k_x\hat{\sigma}_x + k_y\hat{\sigma}_y\right) + \beta k_z\hat{\sigma}_z\right]$$

F. Calavalle *et al.*, Nat. Mater. **21**, 526 (2022)

TELLURIUM: unconventional Rashba-Edelstein effect

Left-handed NW

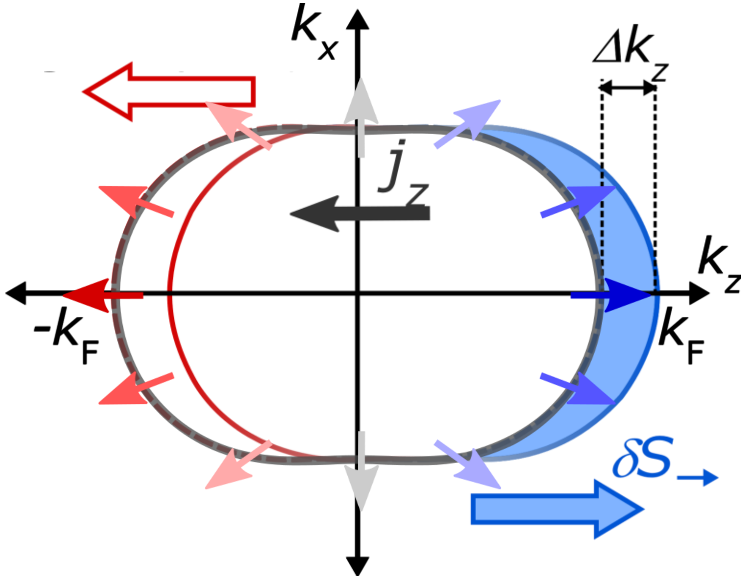

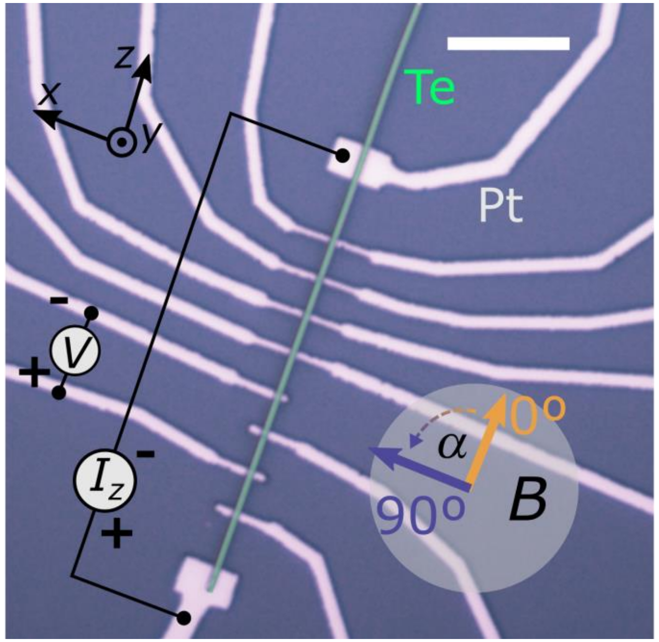

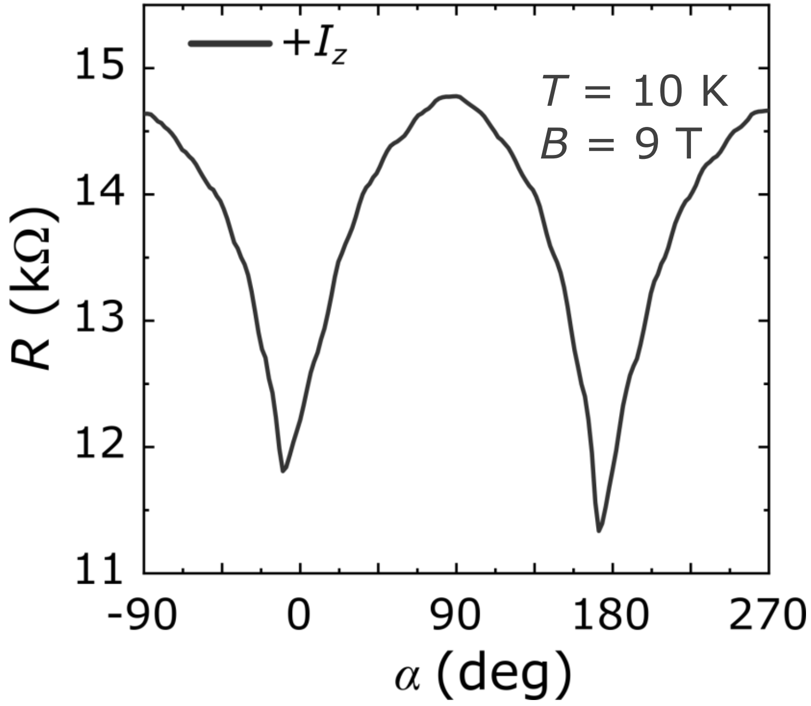

F. Calavalle *et al.*, Nat. Mater. **21**, 526 (2022)

TELLURIUM: unconventional Rashba-Edelstein effect

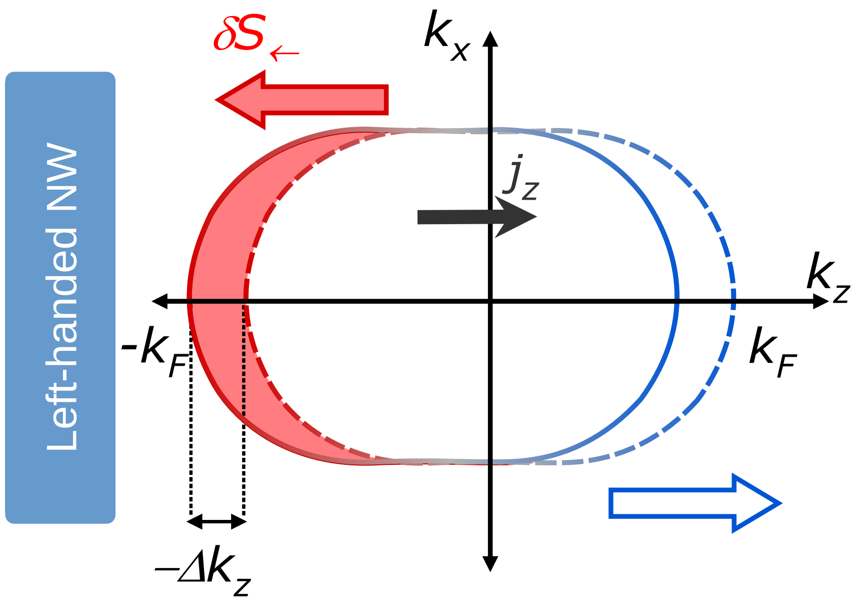

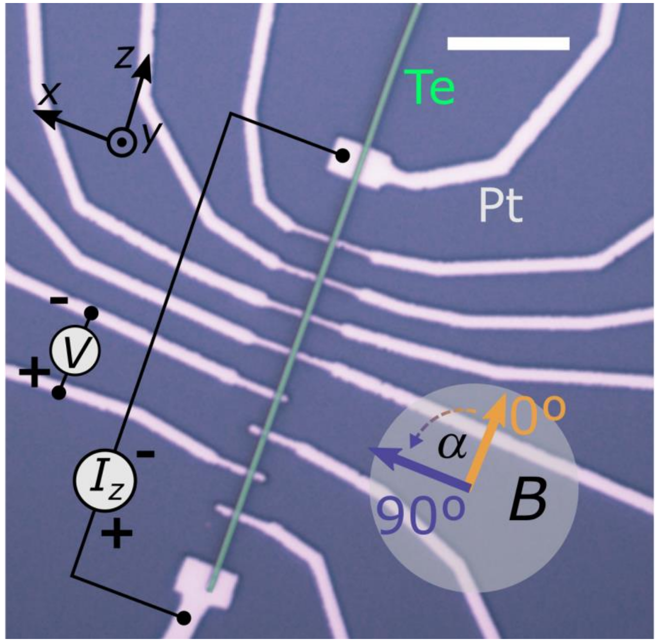

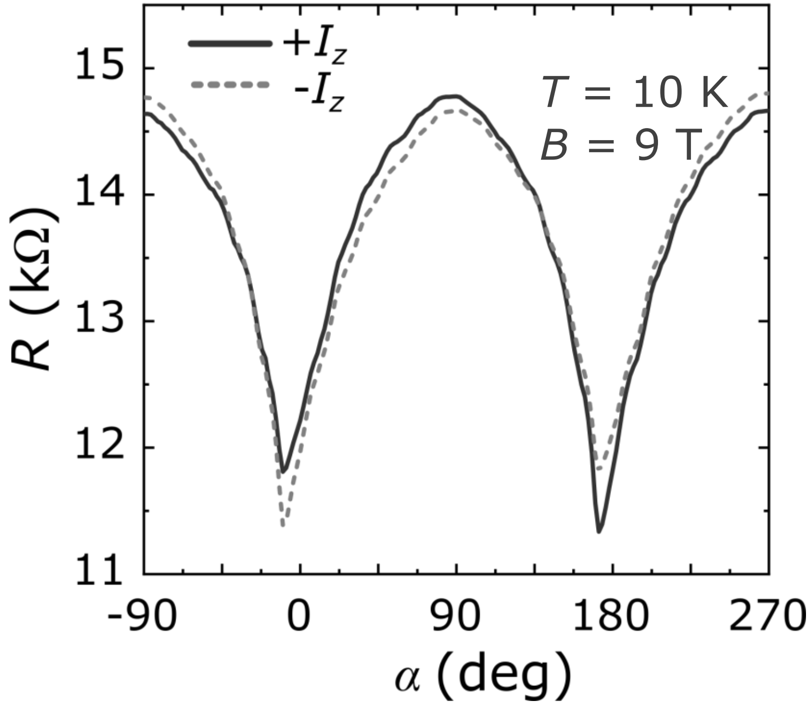

- Resistance depends on the relative alignment between I_z and B
- Unidirectional Magnetoresistance / Bilinear Magnetoresistance / Magnetochiral anisotropy / Non-reciprocal transport

$$R = R_0(1 + \alpha B^2 + \eta j B)$$

F. Calavalle *et al.*, Nat. Mater. **21**, 526 (2022)

TELLURIUM: chirality dependent UMR

$$R^{\text{diff}} = \frac{R(+I_z) - R(-I_z)}{2}$$

Left-handed NW

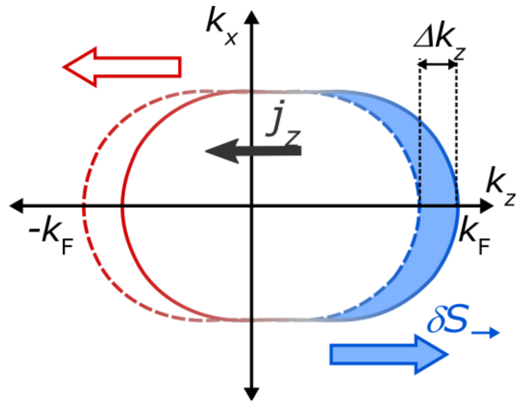

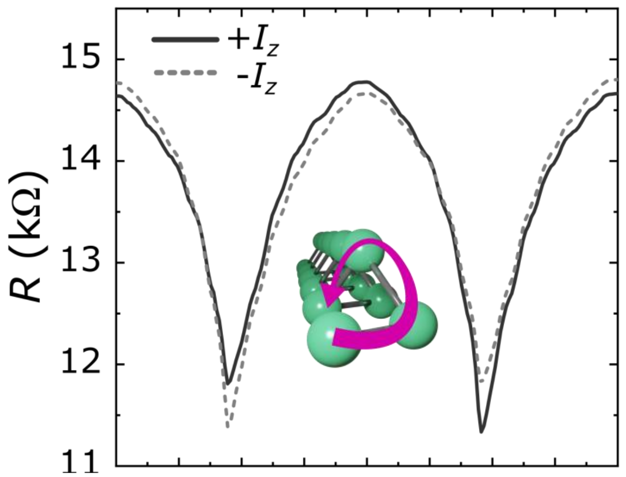

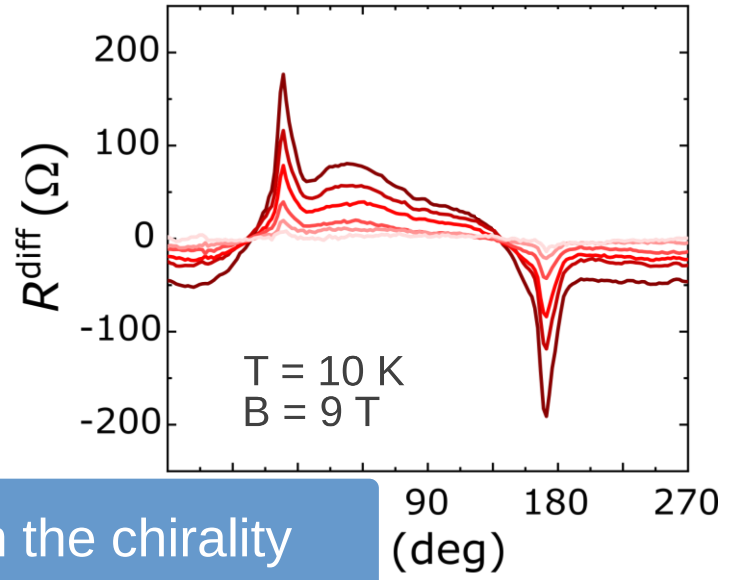

Spin-polarization depends on the chirality

Right-handed NW

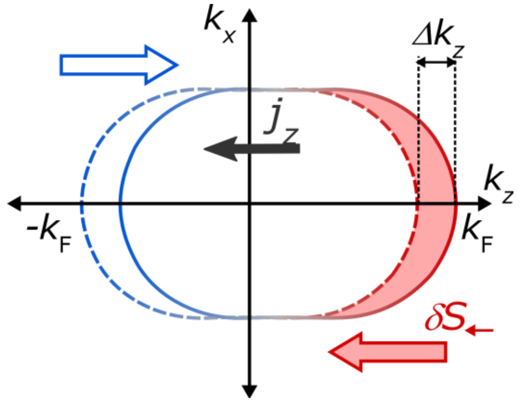

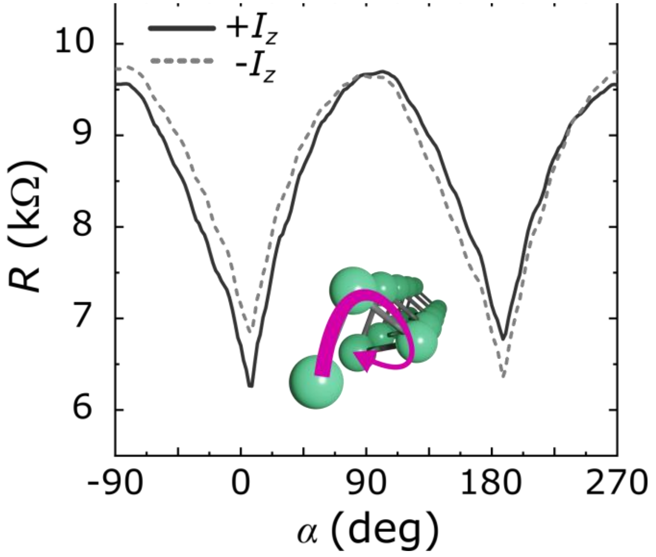

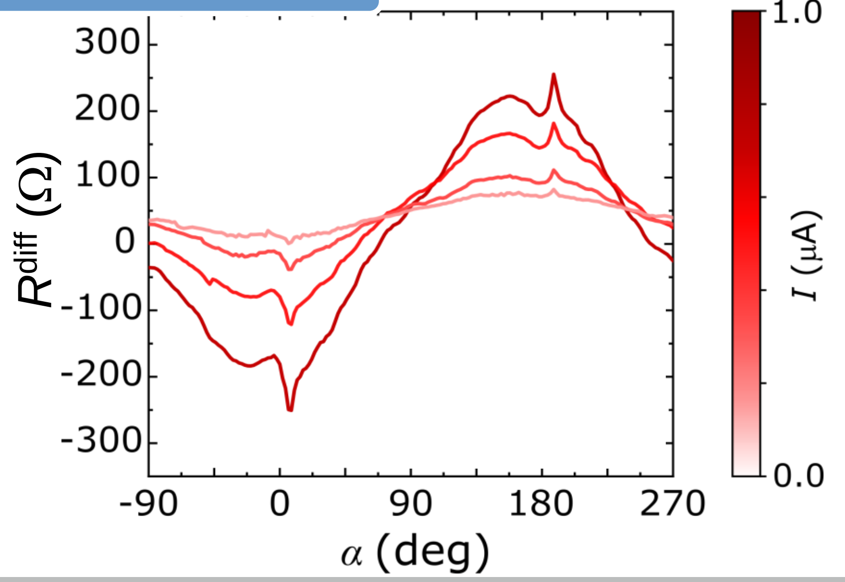

F. Calavalle *et al.*, Nat. Mater. **21**, 526 (2022)

TELLURIUM: UMR quantification

$$\eta = \frac{R_{diff}}{R_0 j B}$$

Material	Spin Texture	Type	η ($cm^2 A^{-1} T^{-1}$)	
Tellurium	Radial	Chiral material	4×10^{-6}	Our work
Ge (111)	Helical	Rashba surface	4.2×10^{-7}	Phys. Rev. Lett. 124, 027201 (2020)
BiTeBr	Helical	Polar semiconductor	3×10^{-8}	Nat. Phys. 13, 578-583 (2017)
SrTiO3	Helical	Rashba surface	4.2×10^{-8}	Phys. Rev. Lett. 120, 266802 (2018)
α- GeTe	Helical	Rashba surface and bulk	7.1×10^{-10}	Nat. Commun. 12, 540 (2021)
Bi_2Se_3	Helical	Topological insulator	5.9×10^{-11}	Nat. Phys. 14, 495-499 (2018)
WTe_2	Helical	Topological semimetal	1×10^{-13}	Nat. Commun. 10, 1290 (2019)
CoPt	Helical	Rashba bulk	5.9×10^{-14}	Phys. Rev. B 107, 094410 (2023)

CONCLUSIONS

Spin-orbit proximity in van der Waals heterostructures

Largest and gate-tunable spin-to-charge efficency

Low symmetry materials provide new spintronic phenomena

Twistronics meets spintronics

Tellurium as a playground for chiral spintronics

ACKNOWLEDGMENTS

ICN2 (Barcelona)



M. Vila J.H. Garcia S. Roche

DIPC (San Sebastian)

F. de Juan

Martin-Luther U. (Halle)


A. Johansson I. Mertig

U. Minnesota


S. Lee T. Low

Charles U. (Prague)



P. Nemec J. Kimák E. Schmoranzerová

FUNDING:

GOBIERNO DE ESPAÑA MINISTERIO DE CIENCIA E INNOVACIÓN

AGENCIA ESTATAL DE INVESTIGACIÓN

EXCELENCIA MARÍA DE MAEZTU

ikerbasque Basque Foundation for Science

THE FRAMEWORK PROGRAMME FOR RESEARCH AND INNOVATION HORIZON 2020

HORIZON EUROPE

MARIE CURIE ACTIONS

"la Caixa" Foundation

intel